Identifying Sources of Elevated Mn at Banks Pumping Plant and the South Bay Aqueduct Using Historical Data (2011-2023)

Report prepared under contract with the State Water Contractors by:

Paul V. McCormick, Independent Consultant

FINAL REPORT JULY 2026

TABLE OF CONTENTS

EXECUTIVE SUMMARY

Manganese (Mn) is a naturally occurring element in raw water used for drinking water treatment. It is highly reactive and can occur in many different forms (dissolved in water, suspended as colloids, adsorbed to organic particles in the water and sediment, and precipitated to surfaces) depending on environmental conditions such as oxygen levels and pH. Therefore, Mn concentrations within a water system are influenced not only by inflow concentrations but also by internal transformations that remove Mn from and release Mn to the water.

Total Mn concentrations in drinking water systems can exceed the U.S. EPA secondary standard of 50 ug/L due to high Mn in the raw water supply and/or the release of Mn stored within the conveyance (raw water) and distribution (finished water) infrastructure. Previous studies have shown that this infrastructure can alternately serve as a Mn *sink* – a location where Mn is removed from the water – and a Mn *source* – a location where Mn is released back to the water – that changes the concentration and forms of Mn relative to that found in the raw water supply.

This report analyzed Mn data collected from 2011-2023 at SWP monitoring sites Clifton Court Inlet (CCI), Banks Pumping Plant (BPP), and Del Valle Check 7 (DV7) to understand how Mn inputs from the Delta are altered by State Water Project (SWP) infrastructure and operations before reaching downstream water utilities. Local hydrodynamic and biogeochemical processes within the SWP likely promote both Mn storage and release depending on environmental conditions. Therefore, the SWP likely functions as a *transformer* of Mn supplied from the Delta as opposed to simply as a *conduit* of this Mn.

The influence of the SWP on Mn concentrations was determined by comparing Mn concentrations at paired upstream-downstream sites, including the following:

1. <u>A comparison of CCI and BPP</u> to assess how Mn levels are affected by processes occurring in Clifton Court Forebay (CCF).
2. <u>A comparison of BPP and DV7</u> to assess how SBA Mn levels are affected by infrastructure (e.g., Bethany Reservoir, the SBA itself) downstream of BPP.

The first set of analyses comparing Mn levels at CCI and BPP concluded that CCF is an important source of Mn within the SWP and a major cause of total Mn exceedances (>50 ug/L) at BPP. The few BPP exceedances attributable solely to Delta (CCI) inflows occurred during the wettest winters when high volumes of Mn-rich water from the Delta are transported quickly through BPP and CCF serves primarily as a conduit for Delta Mn or perhaps even a sink as a result of dilution and particle settling. BPP Mn exceedances attributable to Mn contributions from within CCF were far more common and occurred during all seasons but were often associated with low and normal flow conditions when water retention times in CCF are longer. Furthermore, CCF contributions to BPP total Mn concentrations appear to have increased since 2011, suggesting that BPP Mn exceedances originating in CCF could be more frequent in the future.

The second set of analyses comparing Mn levels at BPP and DV7 concluded that SWP infrastructure downstream of BPP functions as a Mn transformer, a Mn sink, and a source of total Mn exceedances (>50 ug/L) at DV7. Most exceedances at BPP were not associated with exceedances at DV7, indicating that Mn can be stored downstream of BPP. Most exceedances at DV7 were attributable to Mn contributions downstream of BPP, indicating that this stored Mn can be released periodically. And, while BPP exceedances were attributable to both dissolved and particulate Mn, exceedances at DV7 were mostly due to elevated particulate Mn, indicating that Mn is transformed as it is transported downstream from BPP. Various biogeochemical processes (e.g., Mn reduction-oxidation) and hydrodynamic forces (e.g., sediment settling and resuspension) may influence Mn concentrations at DV7. The potential for greater Mn storage and release in the future between BPP and DV7 exists given the increasing trend for Mn concentrations at BPP.

INTRODUCTION

Manganese (Mn) is a ubiquitous, naturally occurring element that is present in detectable concentrations in most surface waters. Particulate Mn in watersheds originates from the geological weathering of Mn-containing rock and soil and is converted to dissolved Mn under anoxic (low redox) and acidic (low pH) conditions that can occur in groundwater and soils. Accordingly, manganese enters streams and rivers in both particulate forms often bound to soil and sediment particles and dissolved forms in subsurface inflows. Hydrologic conditions influence the relative importance of these two fractions, e.g., particulate Mn concentrations typically increase during periods of high suspended particle loads, and transformations between fractions occur slowly in open flowing channels such as the Delta waterways. Within lakes and reservoirs, where water residence times are longer, Mn can be transformed between dissolved (free ions and low molecular weight compounds), particulate (settleable, filterable particles), and colloidal (finer dispersed particles) fractions. These waterbodies also store incoming particulate Mn that accumulates in the bottom sediments and release dissolved Mn from these sediments when they become anoxic.

Elevated Mn levels in drinking water can have both aesthetic and human health impacts. While there are no mandatory limits for Mn in drinking water, the U.S. EPA has established a secondary standard for total Mn of 50 ug/L in finished water as a guideline to avoid aesthetic issues caused by elevated Mn, including water discoloration, staining of household fixtures, and taste issues. This standard is also below levels that are associated with human health effects. The California DDW follows this 50 ug/L standard while also having a customer notification level that was lowered to 50 ug/L from the previous level of 500 ug/L in June 2026. In this report, ***a total Mn concentration >50 ug/L is referred to as a Mn exceedance*** because it exceeds the EPA secondary standard and may prompt a water treatment plant to adjust operations to remove excess Mn from the incoming raw water. The finished water distribution system can also be a source of Mn exceedances due to accumulations of Mn-containing sediments and precipitates within the system that can be released back to the finished water under certain environmental conditions (Brandhuber 2013). Thus, the distribution infrastructure can alternately serve as a Mn sink – a location where Mn is removed from the water – and a Mn source – a location where Mn is released back to the water – that is independent of Mn levels in the upstream raw water source. These terms ***Mn sink*** and ***Mn source*** are used in this report in the same manner, but in reference to the SWP infrastructure that delivers Delta water to downstream SWP contractors.

This report analyzed long-term monthly monitoring data to identify Mn patterns and relationships in the portion of the SWP that includes water-quality monitoring stations at Clifton Court Inlet (CCI), Banks Pumping Plant (BPP), and Del Valle Check 7 (DV7) in the South Bay Aqueduct (SBA) (Fig. 1). These stations encompass a series of waterways and infrastructure that regulate the flow of water from the Sacramento-San Joaquin Delta through the northern portion of the California Aqueduct (CAA) to downstream water users. Major features of the system include the following.

1) Radial gates at CCI control the flow of Delta (Old River Channel) water into Clifton Court Forebay (CCF), a large (2200 acres), shallow (depth <10 ft) reservoir that serves as the forebay for Banks Pumping Plant.
2) Pumping at BPP lifts water from CCF into the CAA.
3) After a short distance (~1 mile), water enters Bethany Reservoir, a small (180 acres) reservoir that serves as the forebay for the South Bay Pumping Plant (SBPP) in addition to being part of the main branch of the CAA.
4) The South Bay Pumping Plant releases water into the SBA, which consists of both pipeline and open channel sections and a water quality monitoring station at DV7 downstream of the open channel.
5) Water from DV7 is delivered to downstream WTP intakes through a pipeline section of the SBA.

Water supplied from the Delta is the principal external source of Mn to this portion of the SWP, with the inflow point at CCI. This report focuses on determining whether Mn concentrations and fractions change as water moves through this portion of the SWP and how these changes may impact water utility operations. A simple static model would predict that the SWP conveys Delta Mn downstream without noticeable changes in concentration or composition, in which case SWP Mn levels merely track those at CCI. However, Mn levels within different parts of the SWP infrastructure are likely affected by local hydrodynamics and biogeochemical processes such as Mn storage and release through particulate settling and resuspension, and dissolution in anoxic zones. Recognizing the potential importance of these processes, an alternative dynamic model is proposed that describes the SWP as a *transformer* of Mn supplied from the Delta as opposed to simply a *conduit* of this Mn. This report examines the applicability of this dynamic model to explain Mn patterns in the SWP.

The monitoring stations included in this analysis span sections of the SWP that include various types of infrastructure and operational characteristics that can affect water quality differently. With this in mind, the analysis was divided into two sections, each of which compared a different segment of the SWP using pairs of upstream-downstream monitoring stations.

1. <u>A comparison of CCI and BPP</u> to assess how Mn levels change once Delta water flows through CCF and is pumped into the CAA. This analysis addresses the question: *Are Mn levels in the Delta a good predictor of Mn levels at BPP?*
2. <u>A comparison of BPP and DV7</u> to assess how Mn levels change after water flows through the CAA and Bethany Reservoir and is pumped into the SBA. *This analysis addresses the question: Are Mn levels at BPP a good predictor of levels in the SBA?*

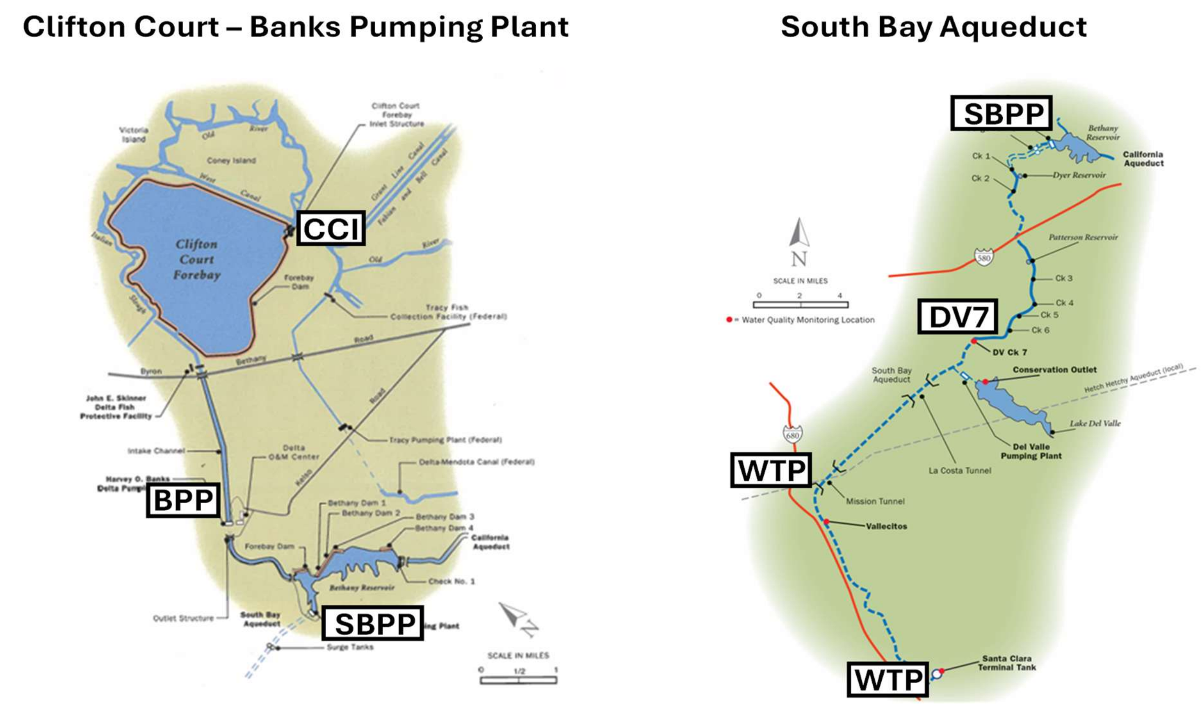

Figure 1 - Major features of the portion of the SWP examined in this study. Locations shown include: CCI – Clifton Court Inlet Monitoring Station; BPP – Banks Pumping Plant Monitoring Station; SBPP – South Bay Pumping Plant (headworks for the SBA); DV7 – Del Valle Check 7 monitoring station; WTP – water treatment plant intakes downstream of DV7. Note the difference in orientation of the two images (as indicated by the directional symbols showing north): the map on the left is oriented in the SW-NE directions while the map on the left is oriented S-N.

GENERAL METHODS

Manganese data and corresponding data for turbidity and TSS (indicators of particle concentrations in the water samples) were downloaded from the Water Data Library website maintained by DWR. DWR currently samples for both dissolved (0.45-um filtered) and total (unfiltered) Mn, but total Mn sampling did not begin until 2011. Therefore, the period of record (POR) used in the analysis was 2011 to 2023, the last year with a full sampling record uploaded to the website. Data were screened for extreme and other suspect values, and a few extreme values were excluded from some analyses to avoid distorting the statistical analysis results. Laboratory results that were reported as below detection were set at half the detection limit.

Box plots (also known as box and whisker plots) were used to show the distribution of the data for each site. These plots are used for the same purpose in the SWP Watershed Sanitary Surveys. The plots consist of a box, which is shows (1) the 50^{th} percentile or median value for the data set (center line); (2) the 75^{th} percentile (Q3) value (top line); and the 25^{th} percentile (Q1) value (bottom line). Two lines or "whiskers" extending from the box encompass all values that fall within the range of +/- 1.5*(Q3-Q1). Values that fall outside the whiskers are labeled as outlier or extreme values and are shown as individual data points.

Temporal (inter-annual, monthly) patterns in the data were identified using LOESS (locally estimated scatterplot smoothing), a non-parametric regression method that fits a smooth curve through the data using local weighted regression. LOESS fits a regression to the moving central tendency of the data rather than assuming a single global relationship and, therefore, is able to identify complex patterns that cannot be revealed using standard linear and non-linear regression methods. LOESS results were useful for indicating general upward or downward trends in Mn concentrations during the POR as well as variations that were associated with shifts between wetter and drier periods. Stepwise regression was performed separately using annual means for each site to test the statistical significance of these two patterns using two predictors: year and annual (CY) BPP flow (an indicator of wetness). The presence of significant directional trends in Mn concentrations and associated variables including turbidity and TSS during the POR was further examined for each site using the Mann-Kendall (MK) Trend Test, a nonparametric test that detects increasing or decreasing trends in time series data.

The strength of relationships between total Mn and other variables was determined using linear regression and, when scatterplots indicated a non-linear relationship, polynomial regression with both a linear and quadratic coefficient included in the model.

RESULTS SECTION 1: CCI vs BPP and the influence of CCF

Relevant CCF Characteristics

Biogeochemical processes within large shallow reservoirs like CCF can modify the water chemistry of Delta inflows that reach BPP, but this influence depends on water residence time and, specifically, the degree of water short circuiting through the reservoir. Delta water enters CCF from the Old River Channel through CCI in the southeast corner of the forebay and travels across the forebay to the outlet channel supplying BPP on the southwest side (Fig. 2). Short circuiting of flow between CCI and the outlet channel (Shrestha and Adil, 2019) reduces the residence time of water in CCF below what would be expected based on the forebay's volume relative to BPP pumping volumes, and the intensity of short circuiting intensifies as inflows through CCI increase (see Fig. 11 and 12 in Shrestha and Adil, 2019). For example, MacWilliams and Gross (2013) predicted average water residence times of about 9 days under low flow conditions and about 4 days under moderate flow conditions. Thus, the overall influence of CCF on water quality at BPP likely decreases with increasing flow through the forebay. These investigators also predicted that water residence time varies considerably within CCF with the longest retention times in the northern and eastern parts of CCF. Therefore, from a biogeochemical perspective, residence time in CCF is not a single number but rather a distribution of values based on hydrodynamic conditions at different locations within the forebay.

Manganese Patterns

Data Distribution. There were 143 paired monthly samples for CCI and BPP during the POR 2011-2023. The range of monthly concentrations for total and dissolved Mn was similar for CCI and BPP, but with a pattern of higher concentrations at BPP (Fig. 3). Median total Mn was higher (37 ug/L) at BPP than CCI (30 ug/L) as was the upper range of data (the "whisker") excluding outliers. The location of the 75th percentile (upper line of the "box") in relation to the 50 ug/L exceedance threshold shows that total Mn exceedances occurred more than 25% of the time (exact frequency = 27%) at BPP compared with less than 25% of the time (exact frequency = 18%) at CCI. Several outliers as high as ~200 ug/L (and a value of 490 ug/L at CCI) occurred at both sites. Note that the extreme value of 490 ug/L was omitted from statistical analyses below due to its undue influence on regression results. Dissolved Mn concentrations followed the same patterns as for total Mn although site differences were less apparent.

Interannual Patterns. Total Mn concentrations during the POR varied widely with alternating periods of higher values at the upstream (CCI) and downstream (BPP) sites (Fig. 4), indicating that both the Delta and CCF can be Mn sources to BPP. LOESS-smoothed trendlines indicated that: 1) total Mn is higher at CCI during the wettest years (2017, 2019, 2023); 2) total Mn is higher at BPP during the driest years (2014-2015, 2020-2022); 3) total Mn at BPP trended upward and increasingly exceeded concentrations at CCI during the POR. Stepwise regression using calendar year and the associated annual BPP pumping volume as potential predictors of total Mn found that pumping (an indicator of wetness) was the only significant ($p<0.050$)

predictor at CCI while year was the only significant predictor at BPP. Kendall trend analysis independently confirmed a significant ($p<0.050$) upward trend for total Mn at BPP but not at CCI during the POR. These results indicate that the Delta's (CCI) contribution to BPP Mn is greatest during wet periods and that contributions from internal sources in CCF have become increasingly important over time. The increasing importance of CCF as a Mn source to BPP is further illustrated by plotting the difference between paired monthly BPP and CCI total Mn values (Fig. 5), which shows an increasing frequency of much higher concentrations at BPP compared to CCI. Note that there may be some bias in these analyses as there are more drought years towards the end of the POR, and an updated analysis using data from 2024-2025 (a wetter period) would help to confirm the above patterns and trends.

Monthly Patterns. Missing data during several years prevented the use of inferential statistics (e.g., Kruskal-Wallis Test) to determine whether there were significant seasonal Mn patterns at CCI and BPP, so summary statistics and trend analysis were used instead to evaluate seasonality at both sites. Monthly box plots (Fig. 6) showed: 1) a similar seasonal pattern for both sites with the highest total Mn values during the winter and summer; 2) greater interannual variability in concentrations at BPP during most months; 3) the potential for total Mn exceedances to occur during all months with the exception of November and December at CCI. A closer examination of selected statistics (Fig. 7) showed: 1) similar average (median) concentrations at CCI and BPP for the months February-July and higher median concentrations at BPP for the months August-January; 2) a higher probability of exceedances at BPP during the months August-February. Finally, a comparison of monthly differences in total Mn concentrations between BPP and CCI using LOESS smoothing (Fig. 8) indicated that CCF tends to be a sink for Mn during the winter and a source of Mn during summer and fall. These results indicate that while both the Delta and CCF contribute Mn to BPP, the added contribution from CCF is often responsible for BPP Mn exceedances, particularly during the late summer and fall months.

Manganese fractions. The data set available for this analysis allowed total Mn to be separated into two fractions: dissolved Mn, which is *measured* analytically on a filtered (0.45 um) sample, and particulate Mn, which is *calculated* as the difference between total and dissolved Mn. Examining these two fractions separately is useful for identifying potential Mn sources contributing to total Mn exceedances. For example, typical sources of dissolved Mn include inflows of anoxic groundwater and releases from anoxic waterway sediments while particulate Mn is associated with soil runoff and sediment resuspension during periods of high flows and windy conditions. It is important to note that the analytical distinction between dissolved and particulate fractions does not fully reflect the spectrum of significant environmental Mn forms, which also include various forms of colloidal Mn that are included in either the filtered or unfiltered fractions based on size.

The relationship between dissolved and particulate fractions was poor at both CCI and BPP (Fig 9); the relationship was significant at CCI due to a few mutually high values but with poor goodness of fit (r^2), and there was no significant relationship at BPP. This suggests that the concentration of these two fractions (as well as potential contributions from colloidal Mn to each fraction) are influenced by different environmental factors.

The contribution of these two fractions to total Mn concentrations varied widely among samples at both CCI and BPP with dissolved Mn contributing between <5% to >70% of total Mn (Fig. 10). Seasonally, dissolved Mn tended to be more important at both sites during the winter and less so during the summer (Fig. 11). Both fractions contributed to total Mn exceedances, although the highest total Mn values had a higher particulate fraction, especially at BPP (Fig. 10).

Monthly differences between BPP and CCI for dissolved and particulate Mn (Fig. 12) showed a similar seasonal pattern as for total Mn with CCF tending to be a Mn sink (primarily for dissolved Mn) in the winter and a Mn source in the late summer and fall. CCF was the largest net source of particulate Mn (possibly including larger sized colloidal Mn) during the summer and early fall and the largest net source of dissolved Mn (possibly including smaller sized colloidal Mn) later in the fall and early winter. This pattern was due both to high exports from CCF during the summer and seasonally low imports through CCI during the fall and early winter (see Fig. 6).

<u>Factors affecting Total Mn</u>

Hydrology. As already noted, hydrologic conditions appear to influence total Mn concentrations in this part of the SWP. Polynomial regression was used to identify significant relationships between annual (calendar year) mean total Mn and associated annual BPP pumping volume and revealed different relationships for CCI and BPP (Fig. 13). Total Mn concentrations at CCI were positively related to pumping, with exceptionally high concentrations in two of the wettest years (2017, 2023), and the relationship was linear. Total Mn concentrations at BPP were also high during these two wettest years as well as during the two driest years (2021, 2022), resulting in a parabolic relationship between total Mn and pumping. These divergent relationships reflect the role of CCF as a net source of Mn during low and moderate pumping years and as more of a conduit of Delta Mn during the highest pumping years. This alternating role for CCF is evidenced by the significant relationship between annual BPP pumping and the difference between annual average BPP and CCI Mn concentrations (Fig. 14). Consistent with the previously discussed stepwise regression results, these findings identify the Delta as the primary source of high Mn to BPP in wet (high pumping) years and CCF as a major source in drier (low pumping years) when Delta Mn concentrations tend to be lower.

The same polynomial regression analysis applied to mean annual %dissolved Mn showed no significant relationship to pumping at either site (Fig. 13). This fraction accounted for between 25 and 45% of total Mn during all but the two driest years when it accounted for <20%. Thus, the high total Mn in these driest years was due disproportionately to a high particulate Mn fraction sourced from CCF.

Suspended Particles. The two monthly measures of suspended particulate concentrations – turbidity and TSS – were highly correlated at both sites, although the relationship was strongest at CCI (Fig. 15). Total suspended solids is the more direct measure of suspended matter, but turbidity appears to be a useful proxy for TSS at these sites and has the advantage of being measured using inline meters to provide real-time information on suspended particle concentrations.

Elevated turbidity and TSS should occur during periods of high watershed runoff and sediment resuspension within Delta waterways as well as during periods of wind-induced sediment resuspension within CCF and would be expected to be associated with higher total Mn concentrations due to an increase in particulate Mn. Total Mn concentrations were positively correlated to turbidity and TSS at both sites; however, the relationship was weak at BPP due to many instances where monthly Mn was high and suspended particle levels were comparatively low (Fig. 16). Both the dissolved and particulate Mn fractions exhibited this same pattern (Figs. 17-18), indicating that concentrations of both fractions at CCI increased during periods of high, turbid Delta flows, but were often high at BPP even when turbidity and TSS levels were low. These findings are also consistent with a model where CCF is a conduit for Delta-sourced Mn when Delta inflows (and, correspondingly, turbidity and TSS) are high and an important source of Mn forms not associated with high suspended matter when Delta inflows are lower.

<u>Sources of Total Mn Exceedances at BPP</u>

There were 38 monthly total Mn exceedances at BPP out of 143 monthly samples during the POR (27% of the time). Exceedances occurred every year except for the first 3 years of the POR (2011-2013), with most years having 2-4 exceedances and the years 2017 and 2021 having exceedances in 6 and 7 months, respectively (Fig. 19). During the 2011-2013 period there were 7 months when total Mn >50 ug/L occurred at CCI, indicating that CCF served as a sink that reduced Mn levels below 50 ug/L at BPP during those years. BPP Exceedances occurred in all months and were most frequent in the winter, and summer, and early fall and less frequent in the spring and late fall (Fig. 20).

The likely source of each exceedance (Delta vs. CCF) was determined by comparing the paired total Mn concentrations at BPP and CCI for each exceedance using the following classification.

1. When the CCI value was <50 ug/L, it was assumed that CCF Mn contributions were responsible for the exceedance.
2. When the paired CCI value was greater than the BPP value, it was assumed that Delta Mn contributions were responsible for the exceedance.
3. When the paired CCI value was >50 ug/L but less than the BPP value, it was assumed that both the Delta and CCF contributed to the exceedance.

Most BPP Mn exceedances (30 months) were attributed to Mn contributions from CCF, and an additional 3 monthly exceedances were attributed in part to CCF. By contrast, there were only 5 months where a BPP exceedance was attributed solely to Delta Mn contributions. BPP exceedances attributable to CCF occurred every year from 2014-2023 and occurred in all months, while those attributable to Delta inflows occurred only during the winter in the wettest years (2017, 2019, 2023) (Figs. 19-20).

The contribution of dissolved and particulate analytical fractions to BPP exceedances varied substantially, with %dissolved Mn accounting for between 2-69% of total Mn concentrations >50 ug/L. The five months during wet winters when exceedances were attributed to the Delta had the highest total Mn, turbidity, and TSS measured during the POR, and both dissolved and particulate Mn were elevated during these months. Most likely, these events were driven by high watershed runoff carrying Mn to CCI. By contrast, in the 30 months when exceedances were attributed to CCF, turbidity (2-28 NTU) and TSS (2-45 mg/L) spanned the full range of measured values during the POR, suggesting that there are multiple (dissolved, colloidal, particulate) Mn forms exported from CCF that contribute to exceedances under different circumstances. These contributions could result from multiple processes such as: 1) the release of dissolved Mn from anoxic CCF sediments; 2) resuspension of sediment-bound particulate Mn due to high winds and flows; 3) formation of particulate Mn due to herbicide applications and subsequent decay of submerged aquatic vegetation (SAV).

CONCLUSIONS: CCI vs BPP and the influence of CCF

This comparison of historical (2011-2023) Mn data for CCI and BPP shows that CCF is an important source of Mn to the SWP and a major contributor to total Mn exceedances (>50 ug/L) at BPP. Furthermore, CCF Mn contributions have increased since 2011, and this statistical trend should be confirmed using more recent Mn data given the implications for future Mn exceedance issues at BPP.

Total Mn concentrations at CCI (Delta inflows) are highest during wet winters and are associated with high concentrations of suspended matter and elevated levels of both particulate and dissolved Mn. All Mn exceedances at BPP attributed to Delta Mn inputs (n=5) occurred during these periods in the months of January through March. Under these high flow conditions, water residence times in CCF are shortened and the forebay serves primarily as a conduit for Delta Mn and possibly even a sink due to processes such as dilution and particle settling.

Far more BPP Mn exceedances (n=30) were attributed to Mn inputs from CCF. These exceedances occurred during all calendar months and were mostly associated with low and normal flow conditions when water retention times in the forebay are longer. These CCF-related events occurred under a wide range of suspended matter concentrations and with varying contributions of particulate and dissolved Mn fractions. These findings support a model where CCF is a significant transformer of Mn entering from the Delta and exports many different Mn forms (dissolved, colloidal, particulate) based on environmental conditions.

Given these findings that CCF is a major source of Mn to BPP, I recommend that further investigation of Mn biogeochemistry in CCF be considered with a focus on how the operation and management of the forebay affects its role as a source of Mn to downstream water utilities.

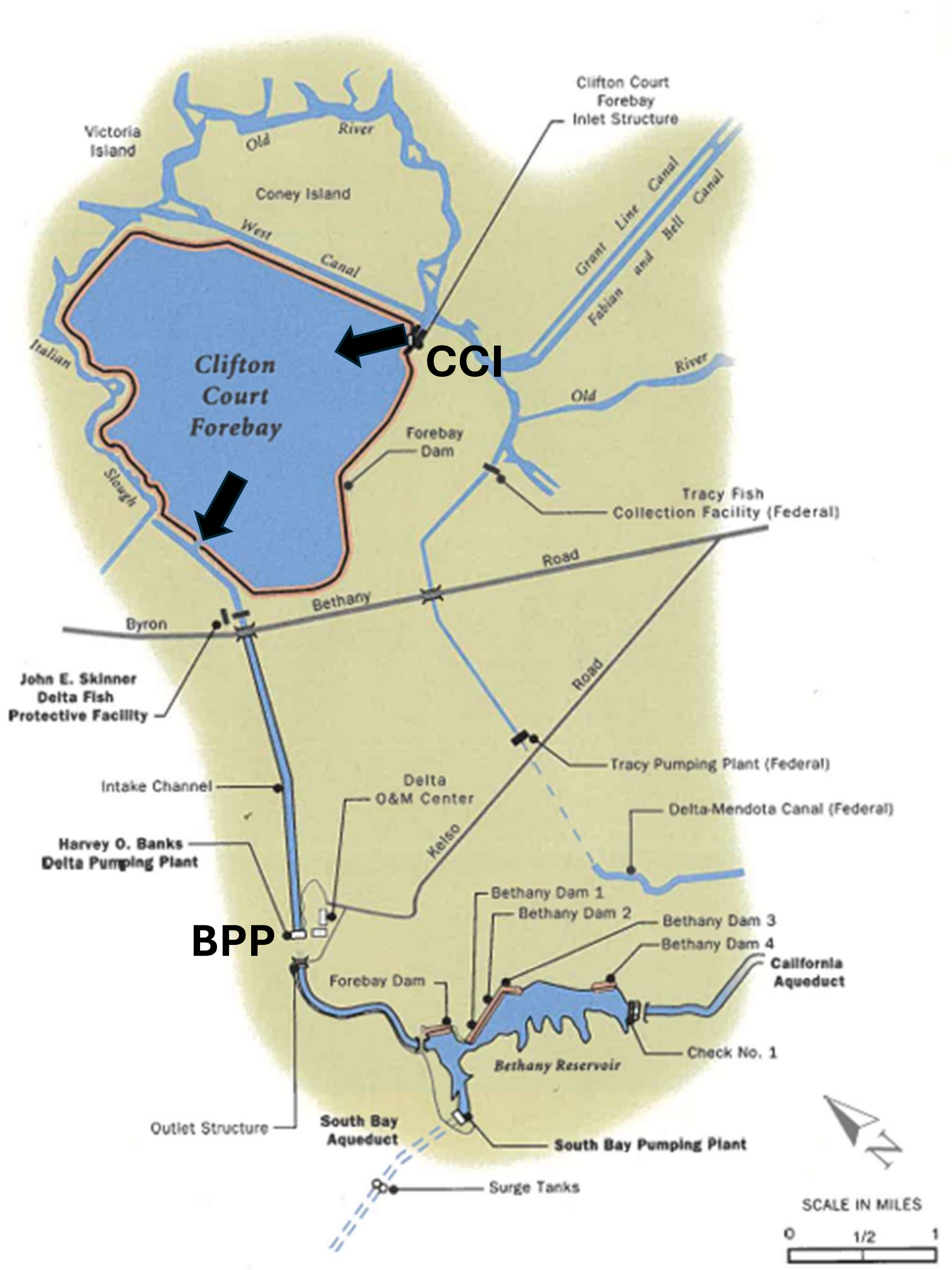

Figure 2 - Map of subject area showing location of monitoring sites CCI and BPP. Arrows show inflow and outflow locations for CCF.

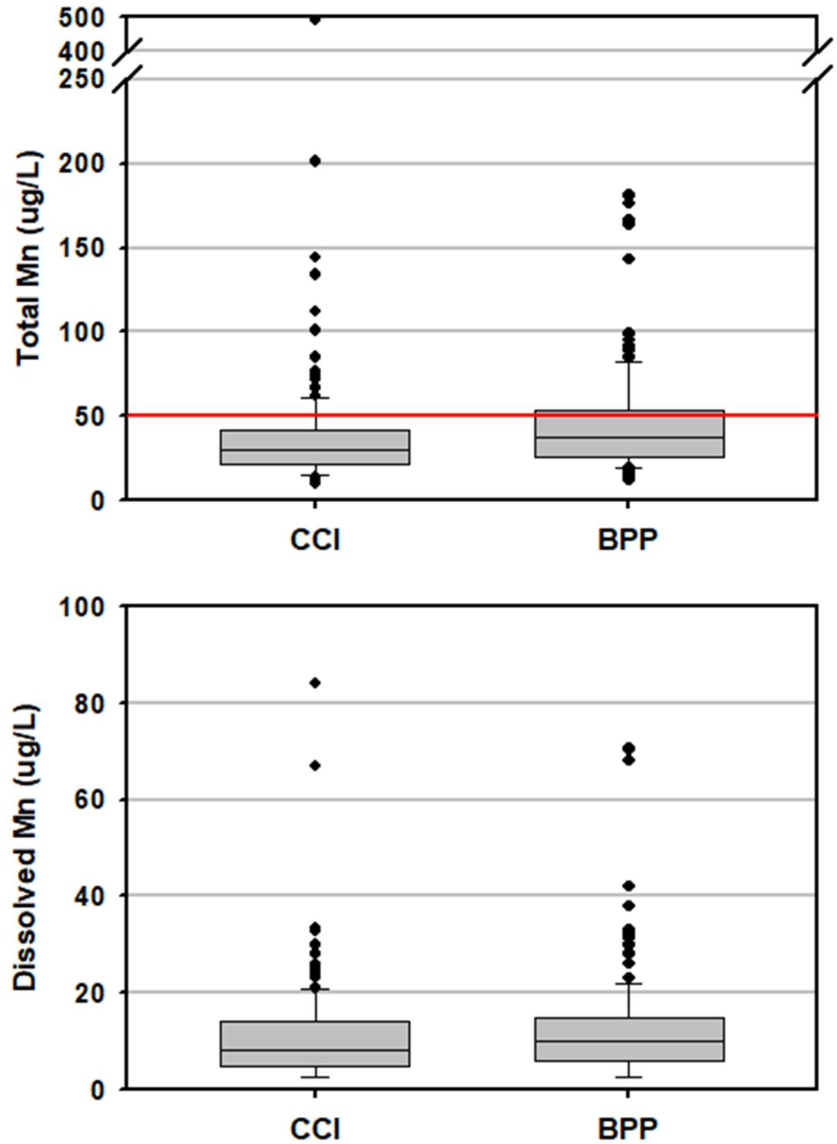

Figure 3 - Box plots of monthly total and dissolved Mn data at CCI and BPP for the period April 2011-December 2023. See General Methods *for explanation of box plot interpretation. Red horizontal line is the 50 ug/L total Mn secondary standard.*

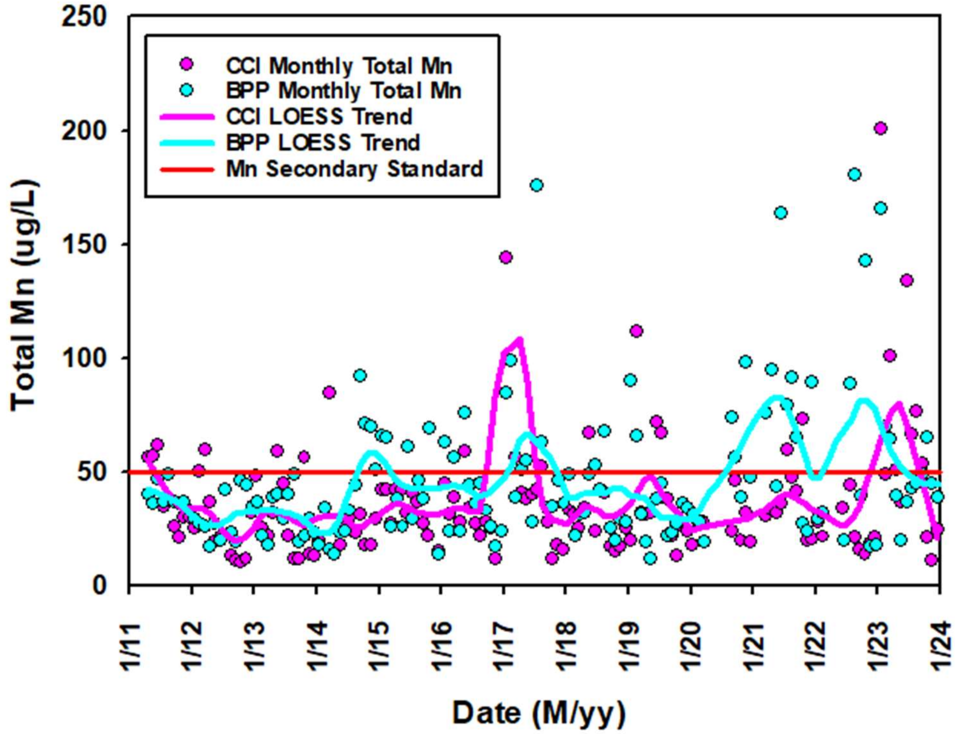

Figure 4 - Time series of monthly total Mn data for CCI and BPP. Trend lines are fitted using LOESS regression. Red horizontal line is the 50 ug/L total Mn secondary standard.

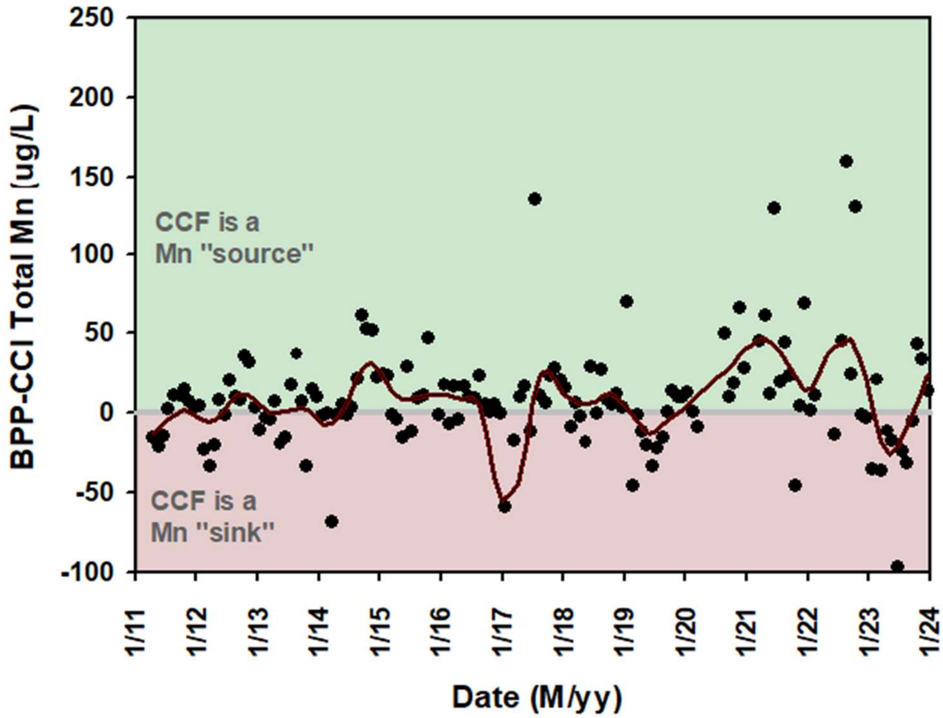

Figure 5 - Time series of the difference between paired monthly total Mn values for BPP and CCI. Positive values (BPP>CCI) indicate that CCF is acting as a source of Mn to BPP while negative values indicate that CCF is acting as a sink for Mn entering through CCI. Trend line is fitted using LOESS regression.

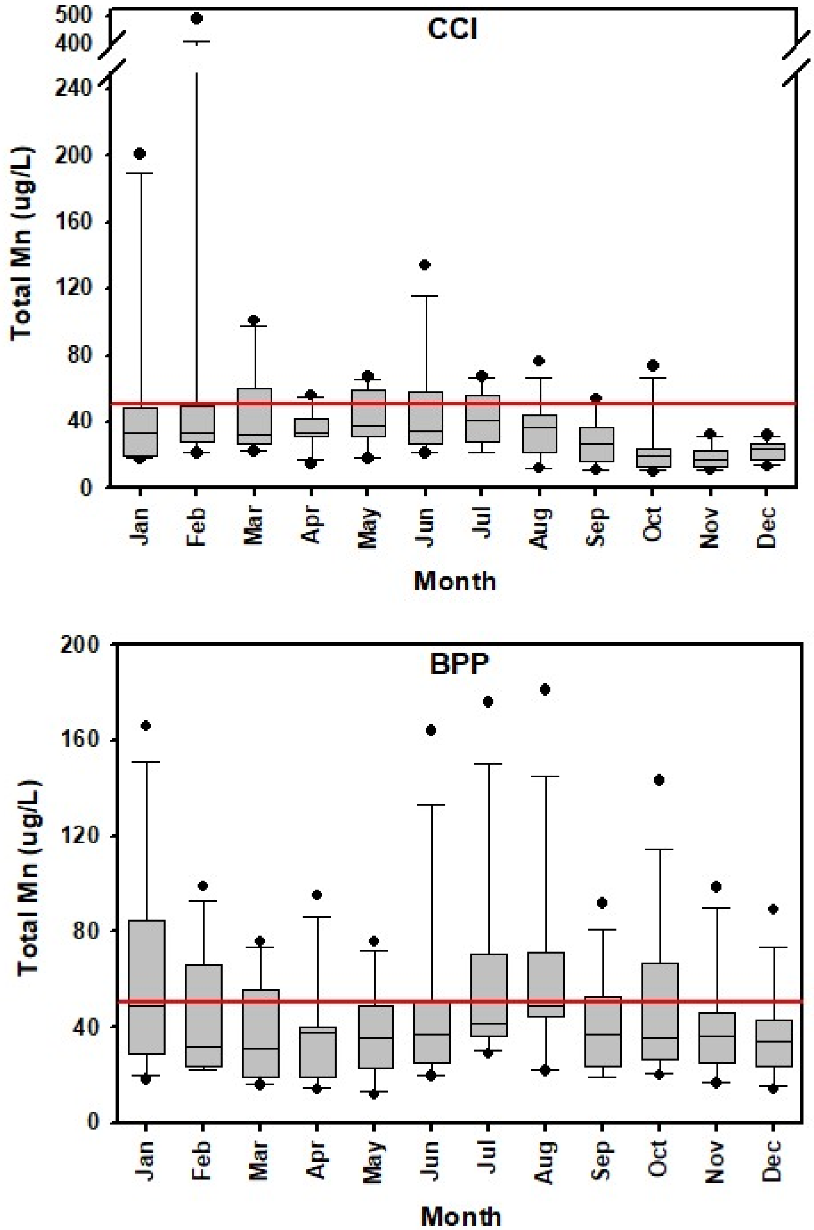

Figure 6 - Box plots of monthly total Mn data at CCI and BPP for each calendar month. See text for explanation of box plot interpretation. Red horizontal line is the 50 ug/L total Mn secondary standard.

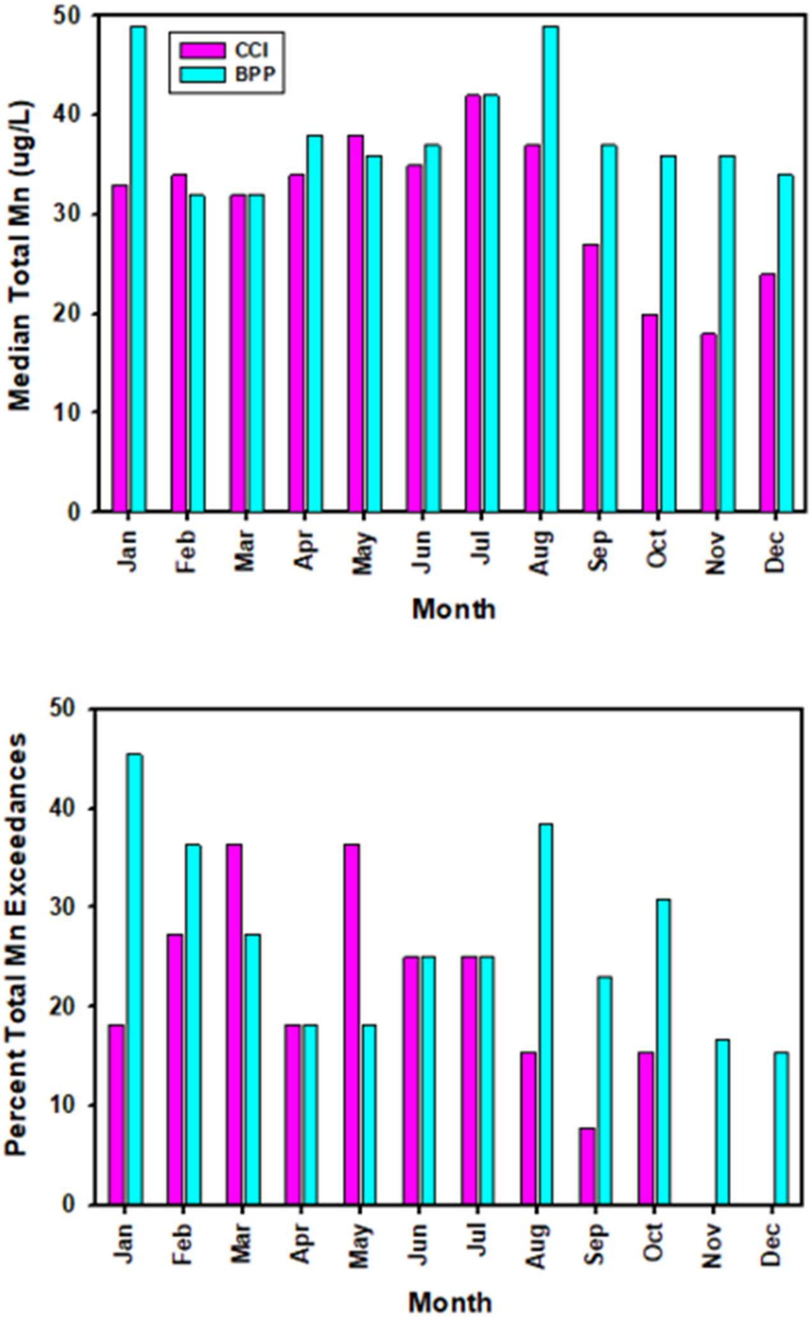

Figure 7 - Median total Mn concentrations and the percentage of years when exceedances (total Mn >50 ug/L) occurred during each calendar month at CCI and BPP.

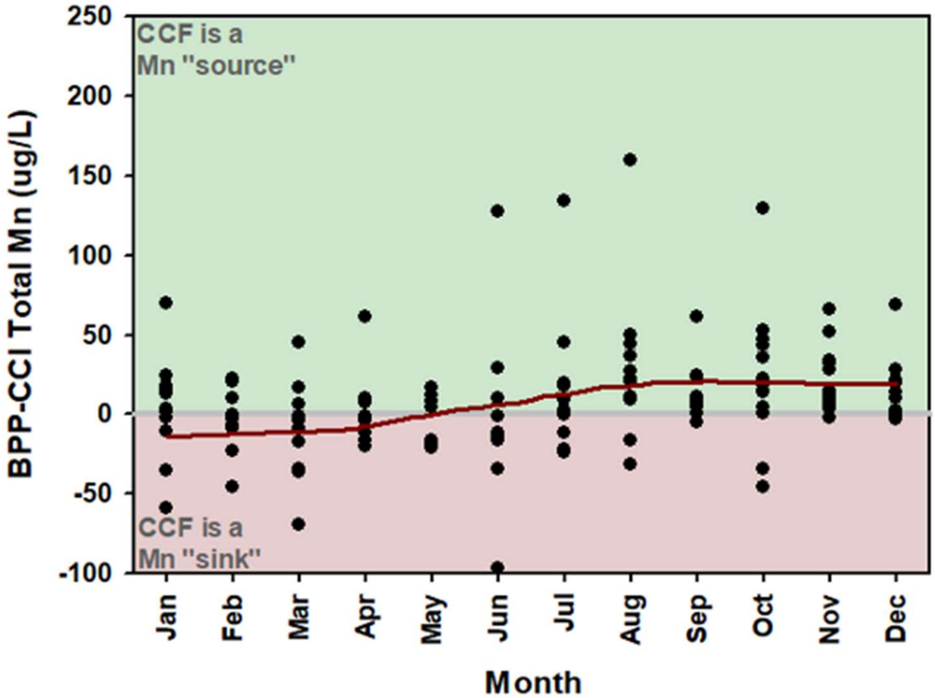

Figure 8 - Differences between paired monthly total Mn values for BPP and CCI for each calendar month. Positive values (BPP>CCI) indicate that CCF was acting as a source of Mn to BPP while negative values indicate that CCF was acting as a sink for Mn entering through CCI. Trend line is fitted using LOESS regression.

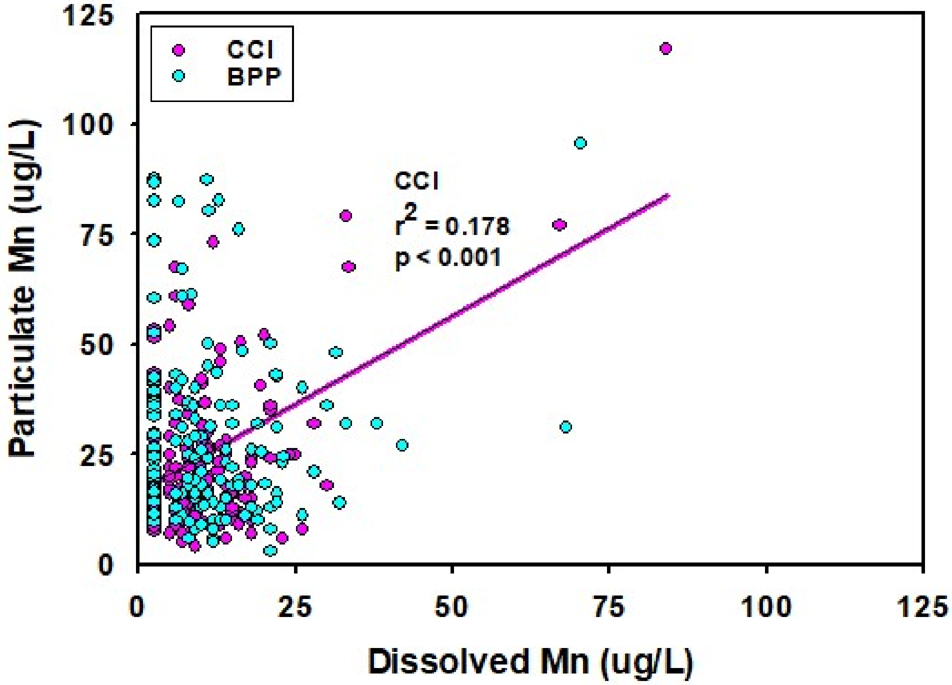

Figure 9 -Paired monthly dissolved (measured) and particulate (calculated) Mn concentrations for CCI and BPP. Line shows a significant relationship for CCI. The relationship was not significant at BPP.

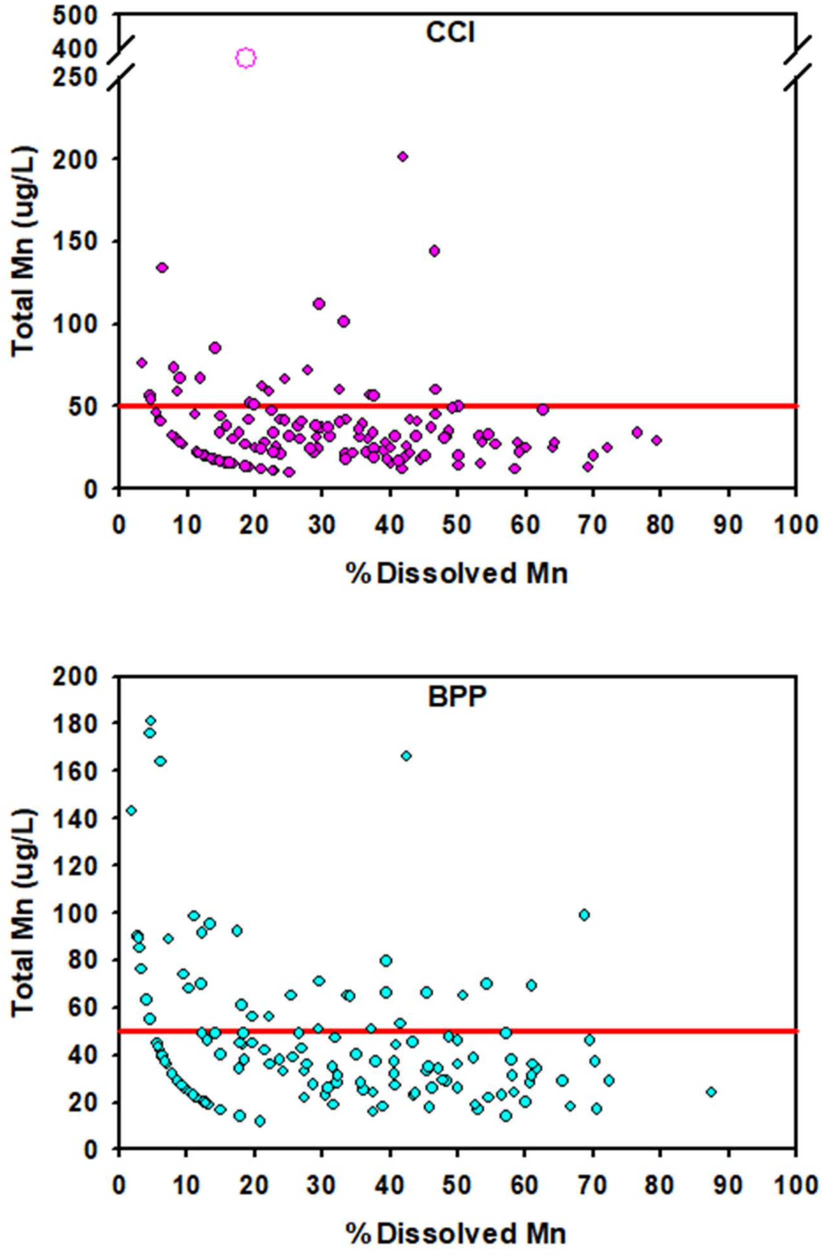

Figure 10 - Percentage contribution of dissolved Mn to total Mn concentrations at CCI and BPP. The CCI graph includes the extreme high value (large open circle) that was not included in statistical analyses. Red horizontal line is the 50 ug/L total Mn secondary standard.

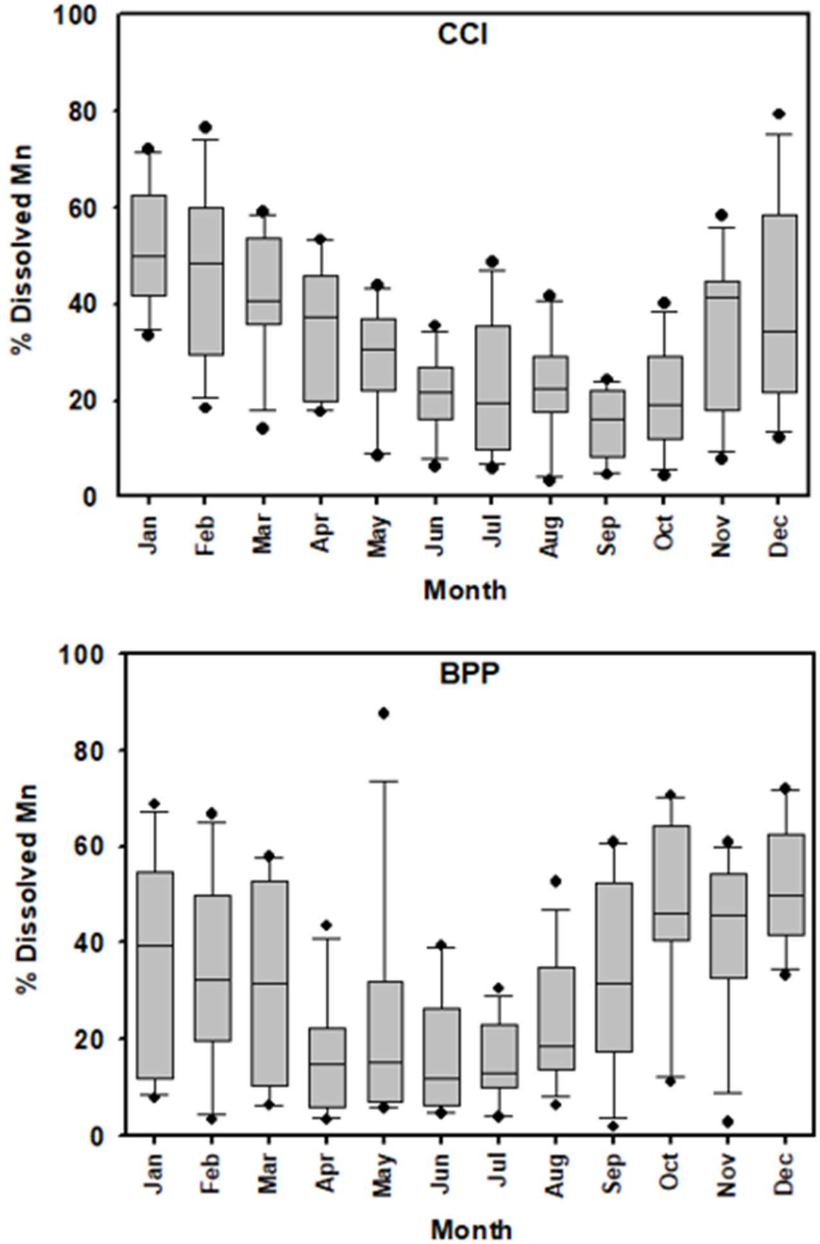

Figure 11 - Box plots of the percentage contribution of dissolved Mn to monthly total Mn concentrations at CCI and BPP for each calendar month. See text for explanation of box plot interpretation.

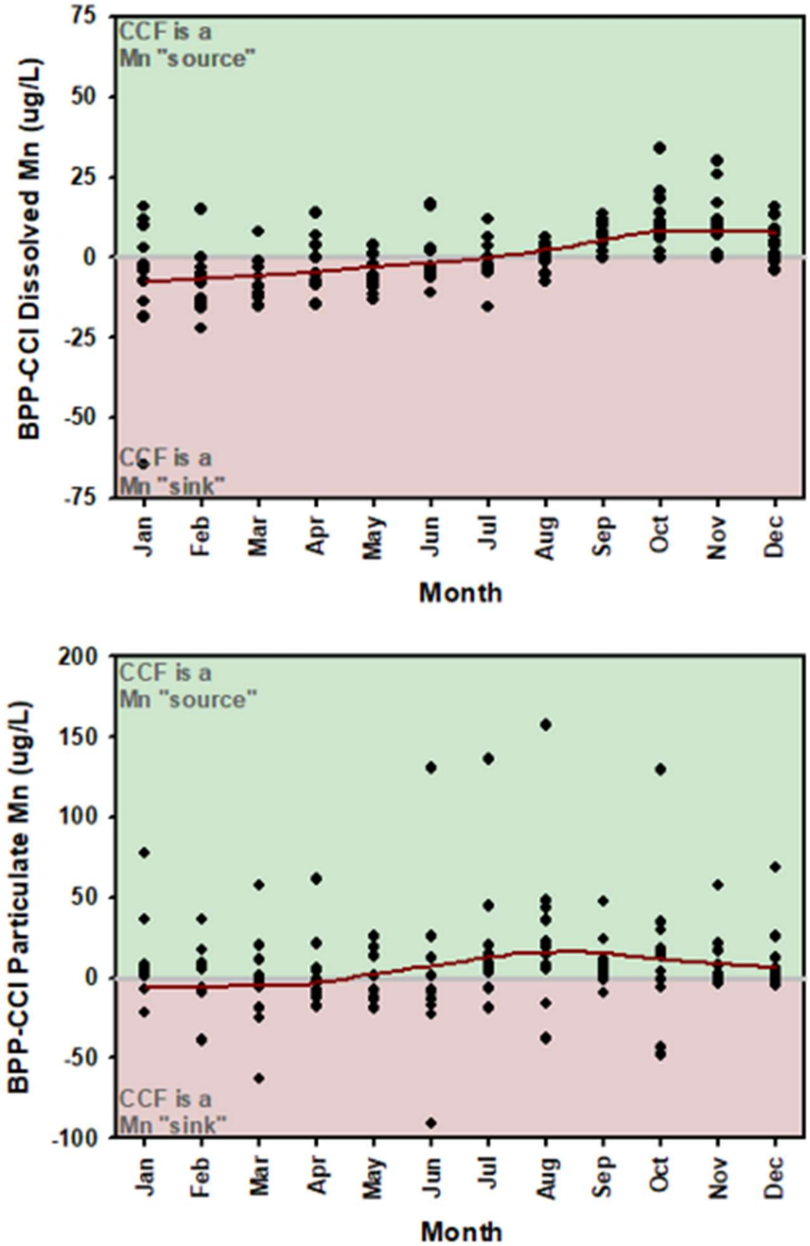

Figure 12 - Differences between paired BPP and CCI values for dissolved (top) and particulate (bottom) Mn concentrations for each calendar month. Positive values (BPP>CCI) indicate that CCF was acting as a source for these Mn fractions to BPP while negative values indicate that CCF was acting as a sink as they enter through CCI. Trend lines are fitted using LOESS regression.

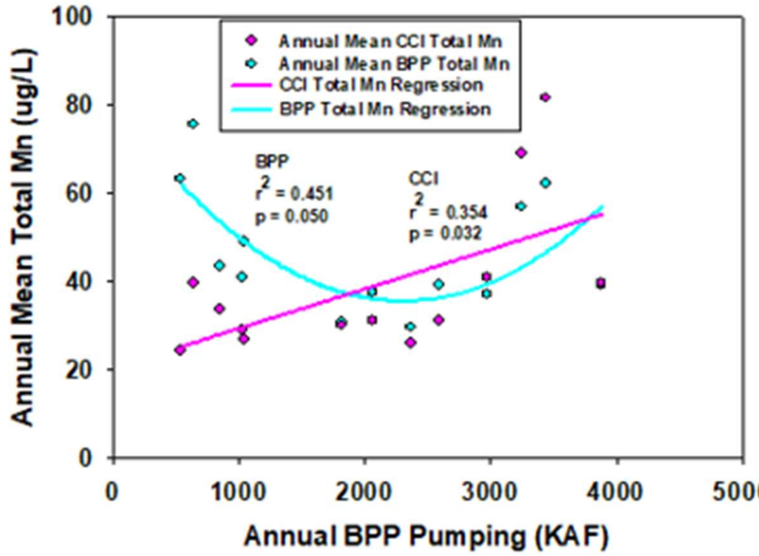

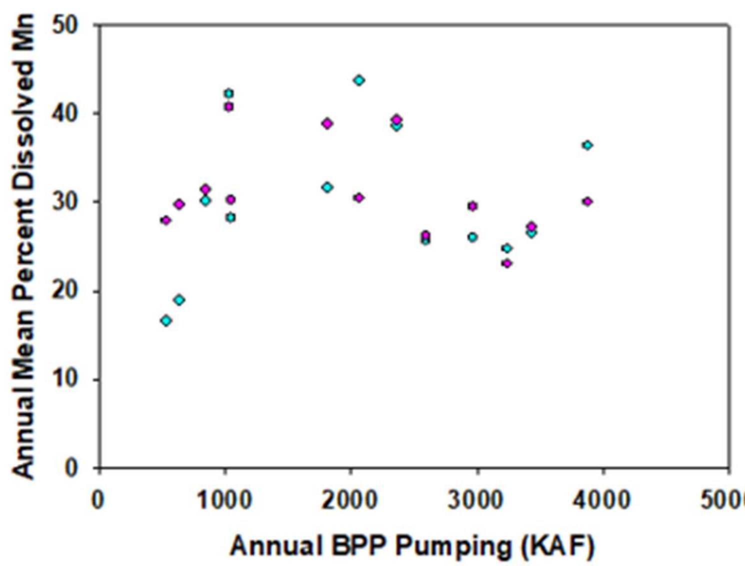

Figure 13 - Relationship between annual mean Mn concentrations and the corresponding annual pumping volume at BPP for total (top) and percentage contribution of dissolved (bottom) Mn at BPP and CCI. The best fit polynomial regression relationships are shown when significant.

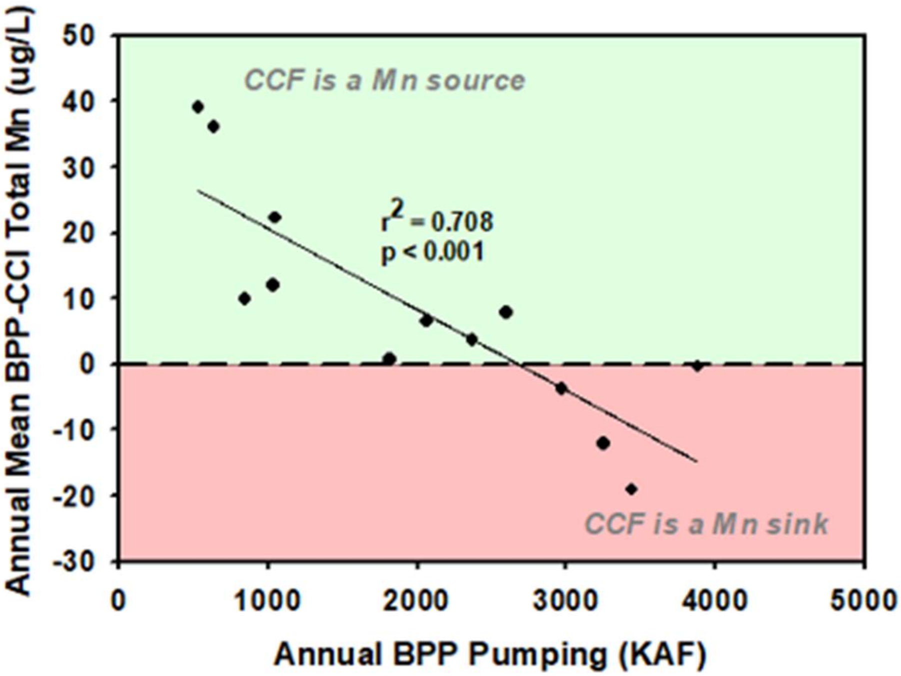

Figure 14 – The relationship between the difference in annual total Mn values for BPP and CCI and the corresponding annual pumping volume at BPP. Positive values (BPP>CCI) indicate that on an annualized basis CCF was a net source of Mn to BPP while negative values indicate that CCF was a net sink for Mn entering through CCI. Line shows significant regression relationship.

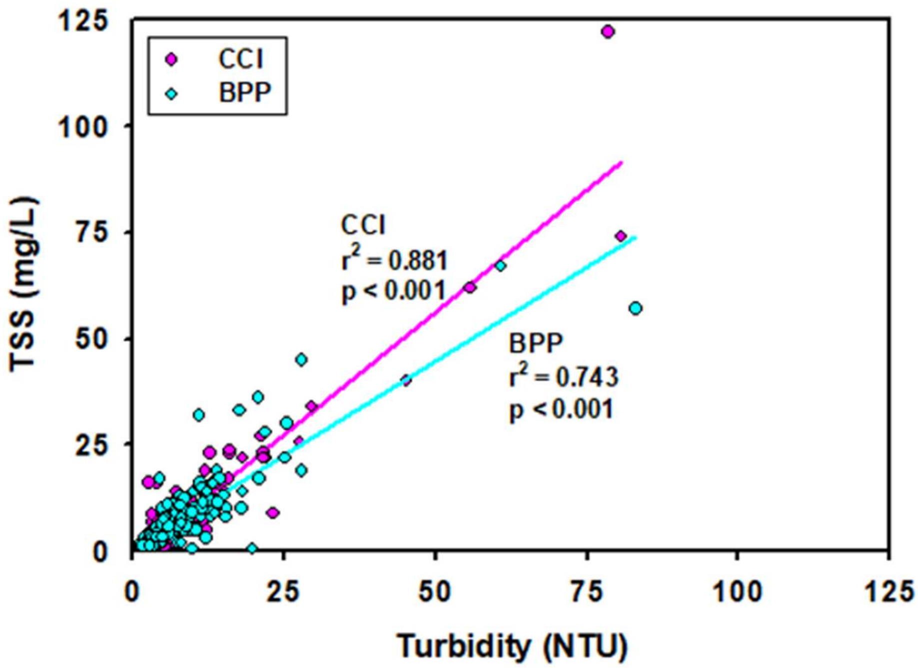

Figure 15 – Relationship between monthly turbidity and total suspended solids (TSS) values for CCI and BPP. Lines show significant regression relationships.

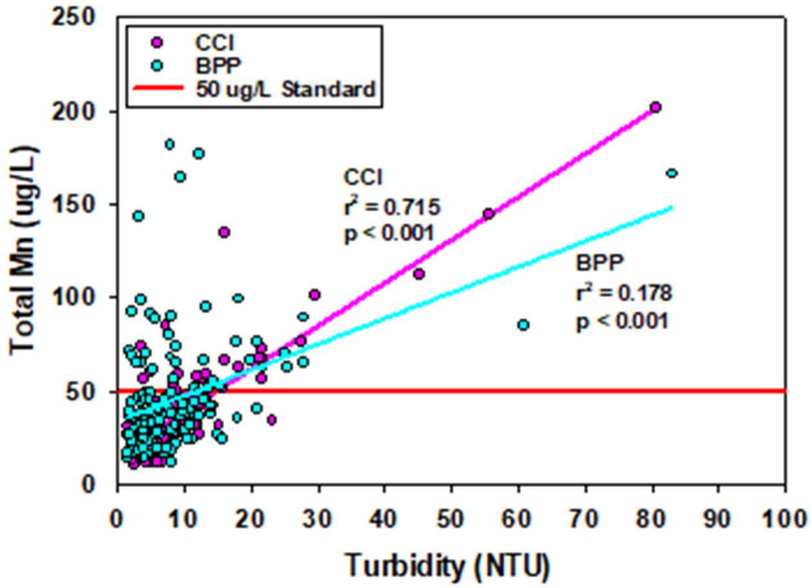

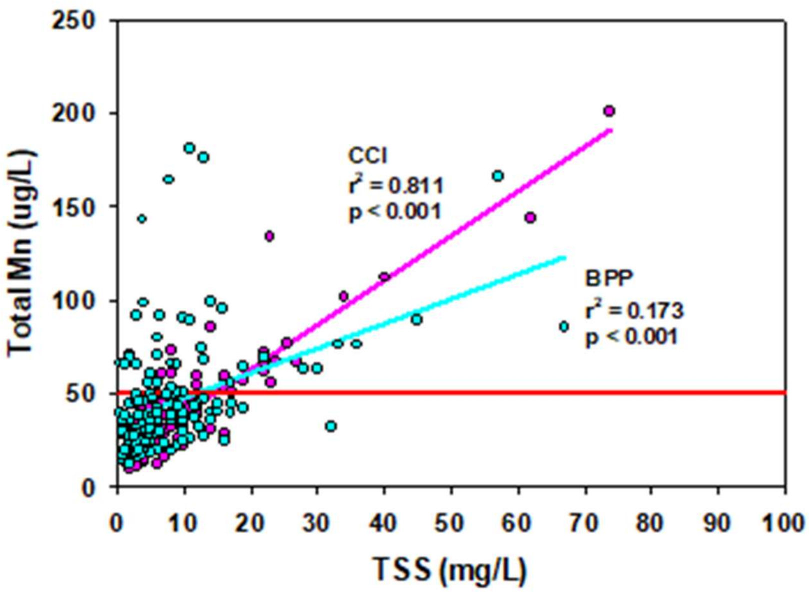

Figure 16 - Relationship between monthly total Mn concentration and measures of suspended matter (turbidity, TSS) for CCI and BPP. Lines show significant regression relationships. Red horizontal line is the 50 ug/L total Mn secondary standard.

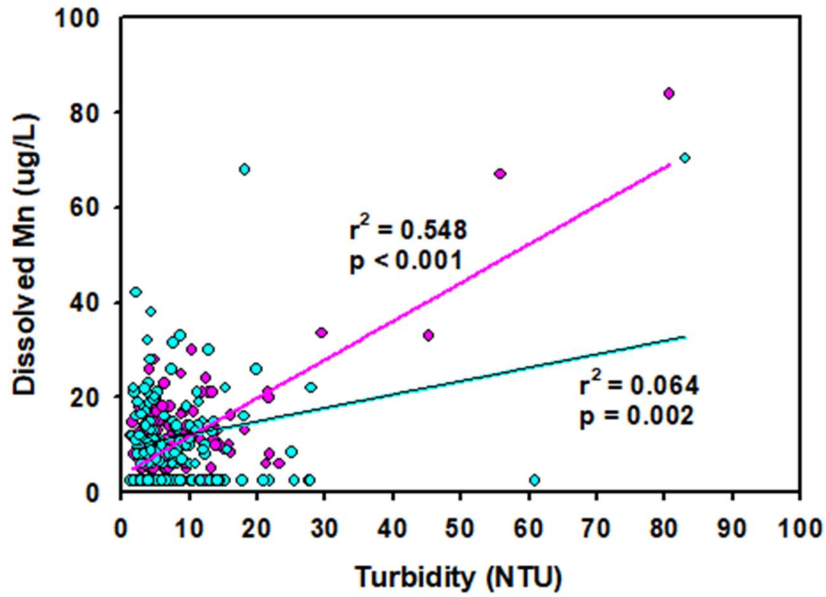

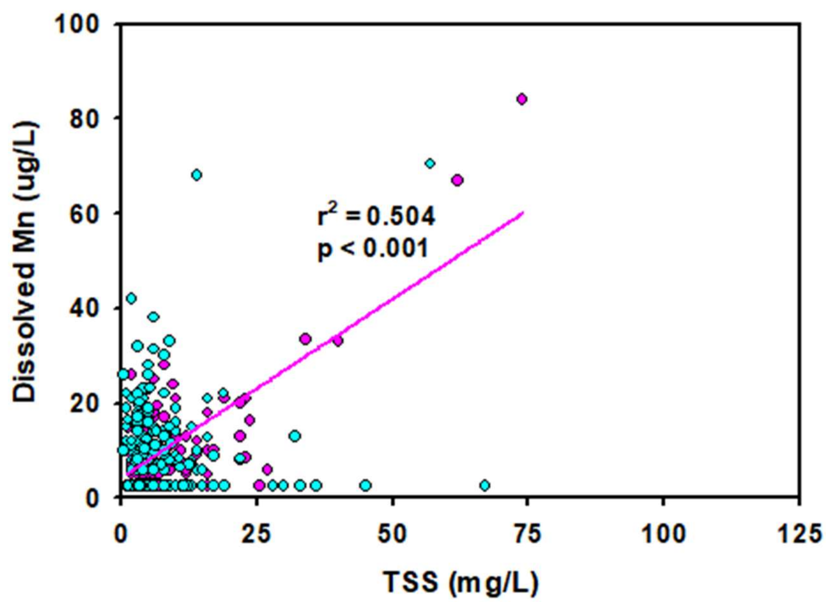

Figure 17- Relationship between monthly dissolved Mn concentration and measures of suspended matter (turbidity, TSS) for CCI and BPP. Lines show significant regression relationships.

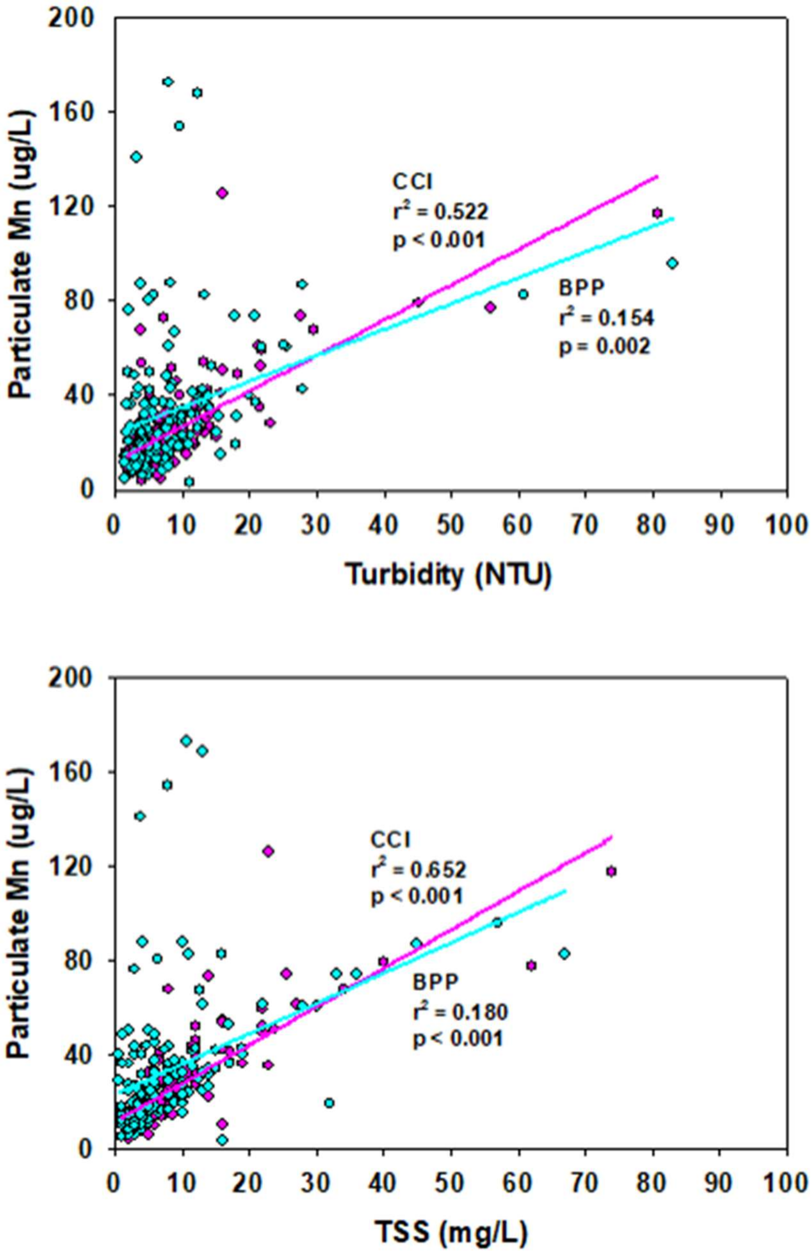

Figure 18 - Relationship between monthly particulate Mn concentrations and measures of suspended matter (turbidity, TSS) for CCI and BPP. Lines show significant regression relationships.

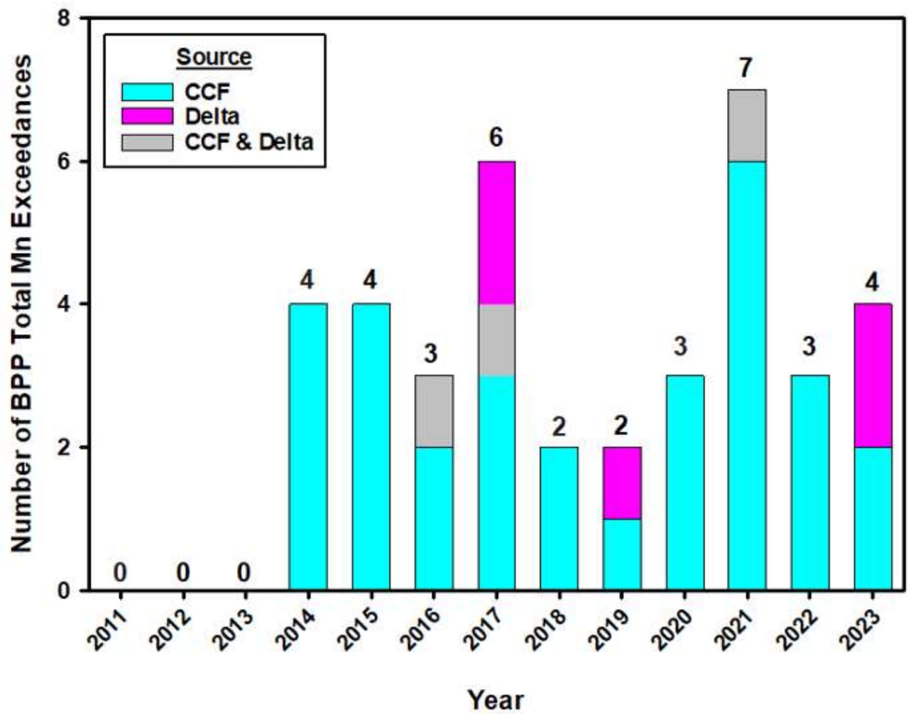

Figure 19 -Number of total Mn exceedances at BPP for each year during the POR. The number of exceedances is shown above each bar. Using the method described in the text, each exceedance was attributed to one of three sources: 1) CCF; 2) the Delta (CCI); 3) contributions from both sources.

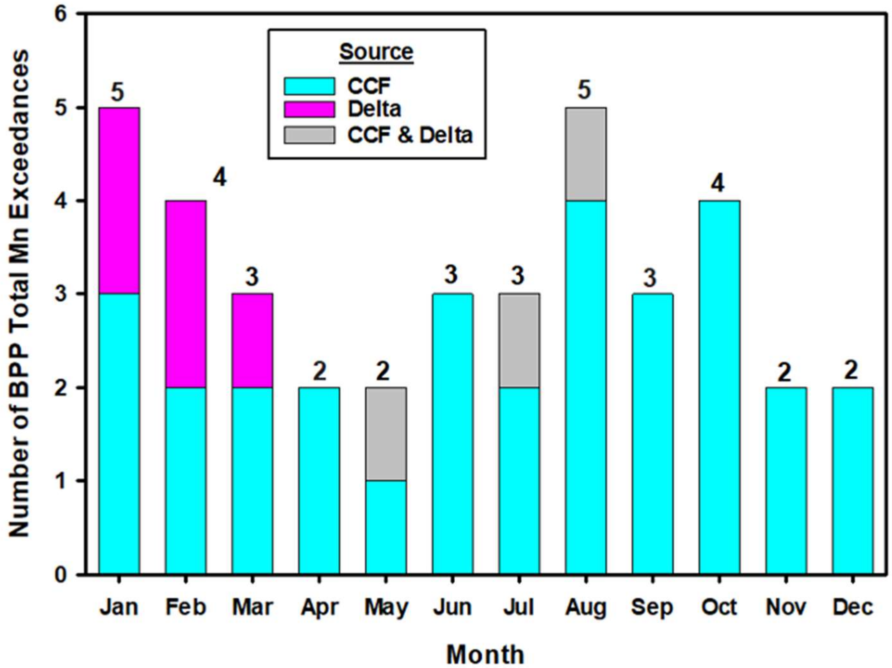

Figure 20- Number of total Mn exceedances at BPP for each calendar month during the period of record. The number of exceedances is shown above each bar. Using the method described in the text, each exceedance was attributed to one of three sources: 1) CCF; 2) the Delta (CCI); 3) contributions from both sources.

RESULTS SECTION 2: BPP vs DV7: The influence of the SWP downstream of Banks

Relevant Characteristics between BPP and DV7

This section focuses on how well BPP Mn concentrations predict those downstream in the SBA. Continuing a major thrust of this report, analyses were conducted with a focus on whether the section of the SWP between BPP and DV7 simply conveys BPP Mn through the SBA or whether it functions in ways similar to CCF (see previous section) by both storing and releasing Mn and thereby influencing downstream Mn concentrations and contributing to Mn exceedances in the SBA.

Major infrastructure between BPP and DV7 is shown in Fig. 21. Water discharged through BPP travels approximately 1 mile through the CAA before entering Bethany Reservoir, which serves both as the forebay for the South Bay Pumping Plant (SBPP) and a conveyance for the CAA. Bethany is a small (180 acre) reservoir that may store and release sediment (and associated Mn) depending on environmental conditions. The SBPP is located near the upstream end of the reservoir and supplies the flow to the SBA. The SBA is a much smaller conveyance than the CAA with a capacity of 300 cfs and consists of 8.4 miles of open channel and 34.5 miles of pipeline and tunnels. The monitoring station DV7 is located at the downstream end of a roughly 7-mile stretch of open channel. A previous study by DWR found this open channel to be biologically active with a high biomass of SAV and algae that cause substantial diurnal pH swings and clogging issues at downstream intakes (Moore and Losee, unpublished technical memo). Sediment retention and resuspension may also occur in the SBA. Two off-channel impoundments, Dyer Reservoir and Lake Del Valle, also supply water to the SBA. Dyer Reservoir is located just downstream of the SBPP and Lake Del Valle is located just downstream of DV7. These inflows are intermittent, and the volumes are small relative to SBPP flows.

Manganese Patterns

Data Distribution. There were 135 paired monthly samples for BPP and DV7 during the POR 2011-2023.The range of monthly concentrations for total Mn was similar for BPP and DV7, but with a pattern of slightly higher concentrations at BPP based on differences in median values (38 ug/L at BPP vs. 30 ug/L at DV7) and quartile ranges (Fig. 22). Approximately 25% of monthly total Mn values at both sites exceeded the 50 ug/L Mn standard, and several outliers ranging between ~75 and 175 ug/L (and a value of 292 ug/L at DV7) indicated that both sites infrequently experienced extremely high total Mn concentrations. Note that the extreme value of 292 ug/L was omitted from most regression analyses below due to its undue influence on regression results. Dissolved Mn concentrations declined substantially as water flowed from BPP to DV7; median concentrations declined from 10 ug/L to below detection (<5 ug/L) and only 18% of the monthly samples at DV7 had dissolved Mn at or above detection. However, extremely high dissolved Mn concentrations occurred during 4 months in different years at DV7 and were not associated with commensurately high concentrations at BPP, indicating a source downstream of BPP.

Interannual Patterns. Total Mn concentrations varied widely at both sites during the POR with multi-year periods of relatively low (few exceedances) concentrations alternating with years having more frequent exceedances (Fig. 23). Monthly concentration differences between the two sites were greatest during periods with the highest concentrations. LOESS-smoothed trendlines for the two sites were similar but with a few periods when concentration trended higher at one site or the other. These results indicate that total Mn concentrations at DV7 generally track those at BPP but can deviate during periods when concentrations are high and exceedances are most likely.

Stepwise regression using calendar year and the associated annual BPP pumping as potential predictors of total Mn found that year was the only significant predictor at BBP but and that neither factor predicted inter-annual variation in total Mn at DV7. Kendall trend analysis confirmed a significant ($p<0.050$) upward trend for total Mn at BPP but not at DV7 during the POR. These results indicate that increasing Mn trends at BPP have not coincided with detectable increases at DV7 and suggest that the infrastructure between these two sites may be storing a portion of the Mn released from BPP.

Differences between paired monthly DV7 and BPP total Mn values (Fig. 24) confirm a pattern where DV7 Mn concentrations generally track those at BPP with the exception of a few periods as already noted above. Individual monthly differences indicate a tendency for modest Mn losses as water flows downstream from BPP (downstream infrastructure acting as a Mn "sink") but also numerous instances when total Mn concentrations are much higher at DV7 (downstream infrastructure serving as a Mn "source").

Monthly Patterns. Missing data during several years prevented the use of inferential statistics (e.g., Kruskal-Wallis Test) to determine whether there were significant seasonal Mn patterns at BPP and DV7, so summary statistics and trend analysis were used instead to evaluate seasonal patterns and differences between the two sites.

Monthly box plots of total Mn concentrations (Fig. 25) showed a seasonal pattern at BPP with highest concentrations during the winter and summer but less predictable seasonality at DV7. Monthly median concentrations were mostly higher at BPP, supporting a pattern of declining Mn concentrations as water flowed between BPP and DV7 (Fig. 26). However, while monthly total Mn exceedances were more frequent at BPP during the winter (Jan-Mar), exceedances were more frequent at DV7 during several other months (Fig. 26). These findings indicate that while BPP is the primary Mn source to the SBA, infrastructure downstream of BPP serves not only as a sink for BPP Mn but also as a Mn source that can contribute to Mn exceedances in the SBA.

Monthly differences and LOESS seasonal trends in total Mn concentrations between DV7 and BPP (Fig. 27) further support the conclusion that while infrastructure downstream of BPP generally conveys or even removes BPP Mn it can also serve as an additional source of Mn that contributes to Mn exceedances in the SBA.

Manganese fractions. There was a substantial shift in Mn fractions as water flowed downstream from BPP to DV7. Whereas dissolved Mn often contributed to Mn exceedances at BPP (see Fig. 8 previous results section), this fraction was rarely (13% of the time) detectable at DV7 and was a major contributor to DV7 total Mn exceedances in only 4 months during the POR (Fig. 28). This shift indicates that biogeochemical processes transform Mn from the dissolved to the particulate fraction as water flows between the two sites.

Particulate Mn concentrations varied considerably but were nearly always the dominant fraction at DV7 (Fig. 28) and the cause of most total Mn exceedances as evidenced by the low contribution of dissolved Mn to exceedances (Fig. 29). It is not clear what factors contributed to the rare occurrence where high (>50 ug/L) dissolved Mn concentrations were a major contributor to exceedances as these events occurred in different months (February, April, August, December) and in years (2015, 2017, 2022, 2023) with different hydrologic conditions. Box plots of DV7 monthly percent-dissolved Mn (Fig. 30) also do not show a clear seasonal pattern.

Monthly differences between DV7 and BPP for the two Mn fractions (Fig. 31) showed that (with a few extreme exceptions) areas downstream of BPP were a net sink for dissolved Mn with greatest losses during the fall and winter. The LOESS trendline for particulate Mn showed little net change between BPP and DV7 on average; however, there was considerable interannual variation for all months, indicating that areas downstream of BPP could be an important particulate Mn sink or source depending on conditions in a given year. Various factors could influence this variation, including flow volumes and other operational conditions and the chemical composition of the particulate Mn fraction (which may include colloidal Mn).

<u>Factors related to Total Mn</u>

Hydrology. Polynomial regression identified nearly identical parabolic relationships between annual (calendar year) mean total Mn and annual BPP pumping volumes for BPP and DV7 (Fig. 32). As mentioned in the previous section (CCI vs BPP), total Mn concentrations at BPP were highest during the highest and lowest pumping years, reflecting variation in Mn inputs from both the Delta (CCI) and CCF. The same pattern existed for DV7 except for lower predicted concentrations in moderate pumping years, supporting the conclusions that BPP is the major Mn source to the SBA and that there is a tendency for Mn losses as water flows between BPP and DV7. These relationships between total Mn and BPP pumping were not associated with shifts in Mn fractions, as indicated by the lack of a relationship between percent-dissolved Mn and flow (Fig. 32); as already noted, the area downstream of BPP consistently had a lower dissolved fraction compared to BPP.

There was no relationship between annual mean total Mn or Mn fractions at DV7 and annual SBPP pumping volumes (Fig 33), indicating that on an annual basis, Mn concentrations in the SBA are controlled by hydrologic conditions at BPP (as shown in Fig. 32). This is consistent with the finding that BPP is the main source of Mn; however, as will be discussed in the <u>Exceedances</u> section below, this general pattern does not mean that conditions downstream of

BPP do not influence SBA Mn levels over shorter timeframes such as the monthly monitoring conducted by DWR.

Suspended Particles. Relationships between suspended particles (turbidity and TSS) and total Mn were weak at BPP due to many instances where monthly Mn was high and suspended particle levels were comparatively low (see Fig. 15 previous section). By contrast, these relationships were significant at DV7 and strongest for TSS (Fig. 34). This relationship was driven by variation in the particulate Mn fraction (Fig. 34), which, as shown above, was generally the dominant Mn fraction at DV7. Therefore, unlike at BPP, TSS and turbidity measurements can be used to indicate the risk of Mn exceedances in the SBA. This relationship is illustrated in Fig. 35, which shows the probability of a total Mn exceedance occurring at different turbidity and TSS levels. For example, TSS concentrations <10 mg/L are associated with a low risk of exceedances, levels of 10-20 mg/L are associated with a moderate risk, and levels >20 mg/L are associated with high risk. Turbidity has a similar predictive ability and has the advantage of being a real-time (i.e., early warning) indicator.

A comparison of turbidity and TSS levels at DV7 and BPP indicate that both BPP and areas downstream can be major contributors of suspended particles (and associated particulate Mn) to DV7 at different times. Levels of both parameters were significantly correlated at BPP and DV7, although the goodness of fit (r^2) was weak for TSS in particular (Fig. 36). Compared to the 1:1 line, the fitted regression lines show a trend of higher turbidity and TSS levels at BPP, consistent with other evidence that areas downstream of BPP tend to be a sink for sediment and Mn. However, these scatterplots show many instances where levels are higher at DV7, consistent with other evidence that areas downstream of BPP can periodically be an additional sediment and Mn source.

A closer examination of turbidity and TSS patterns during the POR further illustrates the importance of areas downstream of BPP as both a sink and a source of suspended matter and associated Mn transported through the SBA. For example, LOESS trend lines for TSS at BPP and DV7 show a similar overall trend for the two sites but with periods where DV7 levels are lower or higher (Fig. 37). This pattern is also evident in the LOESS smoothing of monthly differences in TSS between the sites (Fig. 38), where there are alternating periods when downstream areas simply convey TSS from BPP (difference between sites is near zero), serve as sink for TSS from BPP (negative differential), or provide an additional TSS source (positive differential). Close examination of individual data points indicates that conditions can alternate on a monthly basis during these different periods.

Elevated concentrations of suspended matter and associated Mn in the SBA can be caused solely by inputs from BPP and by contributions from areas downstream of BPP at different times. Hydrologic conditions in the Delta, which influence concentrations at BPP, and operational conditions within the SWP, which may influence sediment deposition and resuspension in the

CAA and SBA, are among the factors that likely determine the occurrence and source of Mn exceedances.

<u>Sources of Total Mn Exceedances at DV7</u>

There were 34 monthly total Mn exceedances at DV7 out of 135 monthly samples during the POR (25% of the time). Exceedances occurred every year except for 2013 and 2018, with several years having only 1-2 exceedances while 2015, 2016, and 2022 experienced frequent exceedances (5-7 months) (Fig. 39). Exceedances occurred in all months except for November and were most frequent during the summer and early fall (Fig. 40).

The likely source of each exceedance (BPP vs downstream areas) was determined by comparing the paired total Mn concentrations at DV7 and BPP for each exceedance using the following classification.

4. When the BPP value was <50 ug/L, it was assumed that downstream Mn contributions were responsible for the exceedance.
5. When the BPP value was >50 ug/L and greater than the DV7 value, it was assumed that BPP contributions were responsible for the exceedance.
6. When the BPP value was >50 ug/L but less than the DV7 value, it was assumed that both BPP and downstream inputs contributed to the exceedance value.

Total Mn exceedances at DV7 were most frequently attributed to Mn contributions downstream of BPP (19 months) whereas BPP contributions were the source in 9 months and both BPP and downstream sources contributed to the exceedance value in 6 months. The contribution of BPP as a source of DV7 exceedances increased during the POR, consistent with the statistically significant trend of increasing total Mn at BPP during the POR presented in the previous (BPP vs CCI) section. Exceedances attributable to areas downstream of BPP were highest in the late summer-fall period and BPP was a contributor during several months, particularly during the summer-fall period.

Most DV7 total Mn exceedances were caused by high concentrations of particulate Mn as the contribution of dissolved Mn to these events was ≤10% with the exception of 4 months already noted when dissolved Mn alone was >50 ug/L and accounted for as much as 76% of total Mn. These 4 months were not associated with especially high dissolved Mn at BPP, suggesting a downstream source, or with unusual hydrology (pumping) or suspended matter concentrations (turbidity and TSS). As already noted, there was a close relationship between the frequency of DV7 total Mn exceedances and higher levels of turbidity and TSS, consistent with the importance of particulate Mn as the primary contributor to most exceedances. These findings contrast with those at BPP, where total Mn exceedances were not consistently associated with a particular Mn fraction or with elevated suspended matter.

Probability that BPP total Mn exceedances will cause DV7 exceedances

There were 37 monthly total Mn exceedances at BPP out of 135 monthly samples during the POR (27% of the time). Exceedances occurred every year except for the first 3 years of the POR (2011-2013), with most years having 2-4 exceedances and the years 2017 and 2021 having exceedances in 6 and 7 months, respectively (Fig. 41). Exceedances occurred in all months and were most frequent in the winter, and summer, and early fall and less common in the spring and late fall (Fig. 42).

Total Mn exceedances at BPP were associated with exceedances at DV7 in 15 months or approximately 40% of the time (see Figs. 41-42); however, in two of those instances the total Mn concentration at DV7 was far higher than at BPP, apparently due to large Mn inputs downstream of BPP. The lack of corresponding DV7 exceedances during the remaining 60% of the time may have been due to Mn losses downstream of BPP and, in some cases, operational conditions such as the SBA being supplied from other water sources such as Dyer Reservoir (note that the Lake Del Valle turn-in is downstream of DV7 and, therefore, not considered in this analysis).

CONCLUSIONS: BPP vs DV7: The influence of the SWP downstream of Banks

This comparison of historical (2011-2023) Mn data for BPP and DV7 shows that both BPP and sections of the SWP downstream of BPP are important sources of Mn to the SBA. Total Mn concentrations at BPP are often higher than those in the SBA (DV7), indicating a net loss of Mn as water flows downstream. However, Mn contributions from the SWP downstream of BPP appear to be the most frequent cause of SBA total Mn exceedances, indicating that downstream areas can also be a Mn source. Therefore, rather than simply being a passive conduit of BPP Mn to the SBA, downstream areas act as an additional reservoir for Mn that influences Mn levels in the SBA.

Several findings indicate that biogeochemical processes downstream of BPP have an important influence on Mn concentrations in the SBA.

1) Total Mn concentrations fluctuated considerably at both sites, but whereas BPP concentrations trended significantly higher during the POR and showed a noticeable seasonal pattern there was no clear trend or seasonality at DV7. These divergent patterns suggest that downstream processes influence the amount of BPP Mn that is delivered through the SBA.

2) Both dissolved and particulate Mn fractions were important components of total Mn at BPP, but dissolved Mn was often undetectable and rarely the dominant fraction at DV7. This shift in Mn fractions indicates that Mn is being transformed as it is transported from BPP to DV7. Consequently, total Mn concentrations and the probability of total Mn

exceedances at DV7 were positively associated with particulate Mn concentrations and levels of suspended matter in the water while no such relationships existed at BPP.

3) Most DV7 Mn exceedances were attributed to inputs of Mn downstream of BPP. While BPP is the major source of Mn to the SBA, BPP total Mn concentrations are often <50 ug/L. Additional Mn contributions from the SWP downstream of BPP can increase Mn concentrations further, resulting in total Mn >50 ug/L at DV7 even when concentrations at BPP are below this level.

4) Most Mn exceedances at BPP were not associated with exceedances at DV7, indicating that the SWP downstream of BPP can function as a Mn sink.

While it is not possible to identify specific biogeochemical processes occurring in this part of the SWP based solely on this analysis of monitoring data, potentially important processes may include: 1) loss of dissolved Mn through transformation to colloidal and particulate forms; 2) adsorption of Mn to sediment particles; 3) sediment settling and resuspension that alternately store particulate Mn in the sediment and release it into the water, possibly in response to changes in SWP flows or other pumping operations.

Discharges through BPP is the main source of Mn to the SWP, and both BPP Mn concentrations and their contribution to DV7 exceedances increased during the POR. Total Mn concentrations at BPP are usually <50 ug/L but further increases in BPP concentrations will increase the potential for Mn exceedances in the SBA. Additionally, higher Mn inputs through BPP may increase downstream Mn storage and release, further contributing to SBA exceedances. As discussed in the previous section (CCI vs BPP), additional investigation is needed to confirm a continued upward trend in BPP Mn concentrations and to identify the sources of this additional Mn.

The section of the SWP between BPP and DV7 appears to strongly influence Mn concentrations in the SBA, but the specific biogeochemical processes and operational conditions that affect this influence are not known. Further investigation of Mn sources (e.g., Bethany Reservoir, the SBA itself) and the factors influencing Mn storage and release (e.g., pumping operations at BPP and SBPP) downstream of BPP may reveal the cause of SBA exceedances and the operational changes or other management measures that could be implemented to reduce Mn impacts to downstream water utilities.

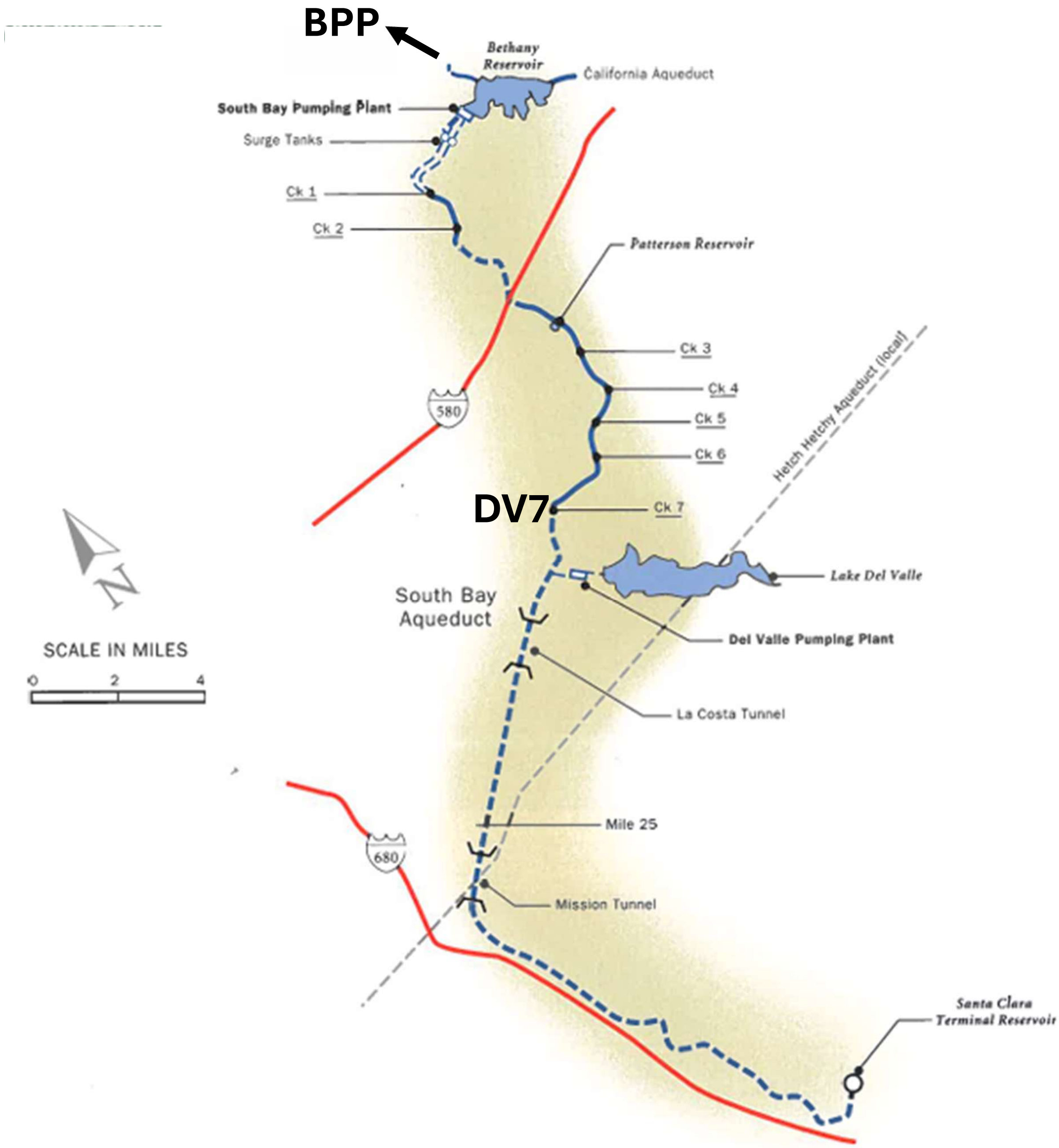

Figure 21 - Map of subject area showing location of monitoring sites BPP and DV7 and associated infrastructure in this section of the SWP. Solid blue lines are open-channel sections of the SBA and dashed blue lines are pipeline sections.

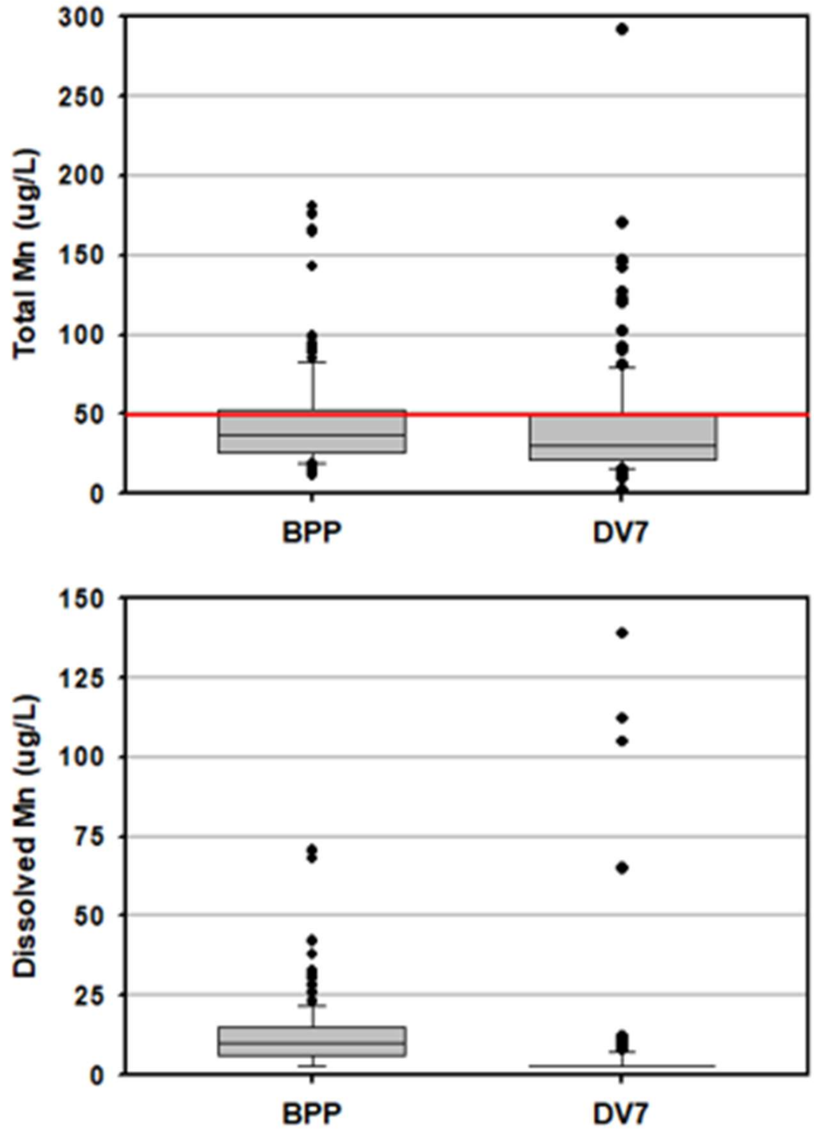

Figure 22 - Box plots of monthly total and dissolved Mn data at BPP and DV7 for the period April 2011-December 2023. See General Methods *for explanation of box plot interpretation. Red horizontal line is the 50 ug/L total Mn secondary standard.*

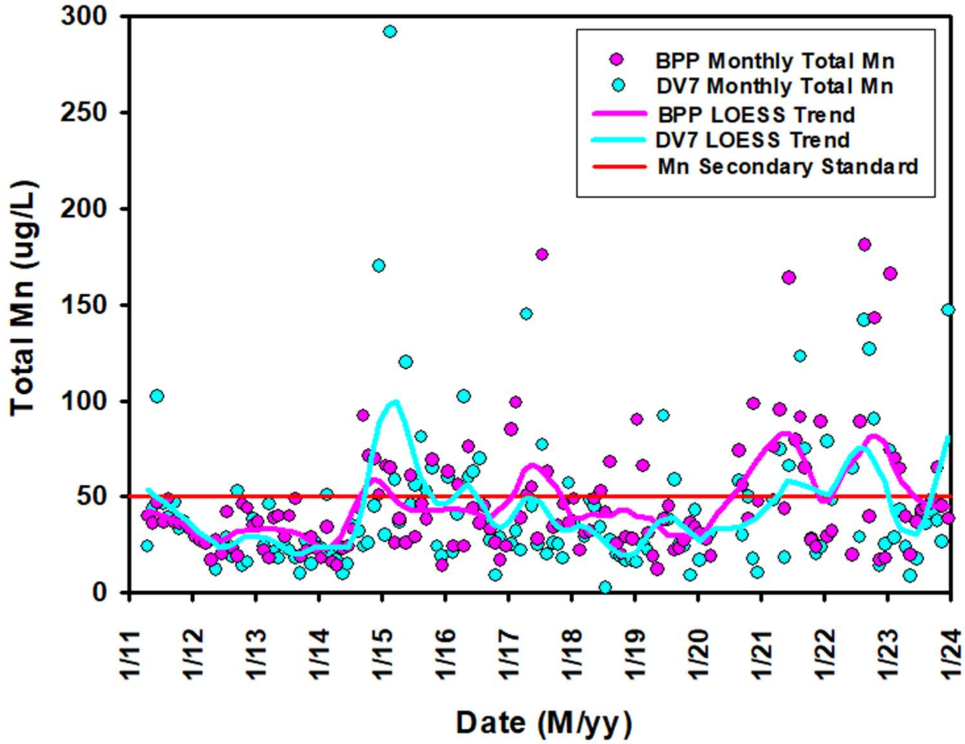

Figure 23- Time series of monthly total Mn data for BPP and DV7. Trend lines are fitted using LOESS regression. Red horizontal line is the 50 ug/L total Mn secondary standard.

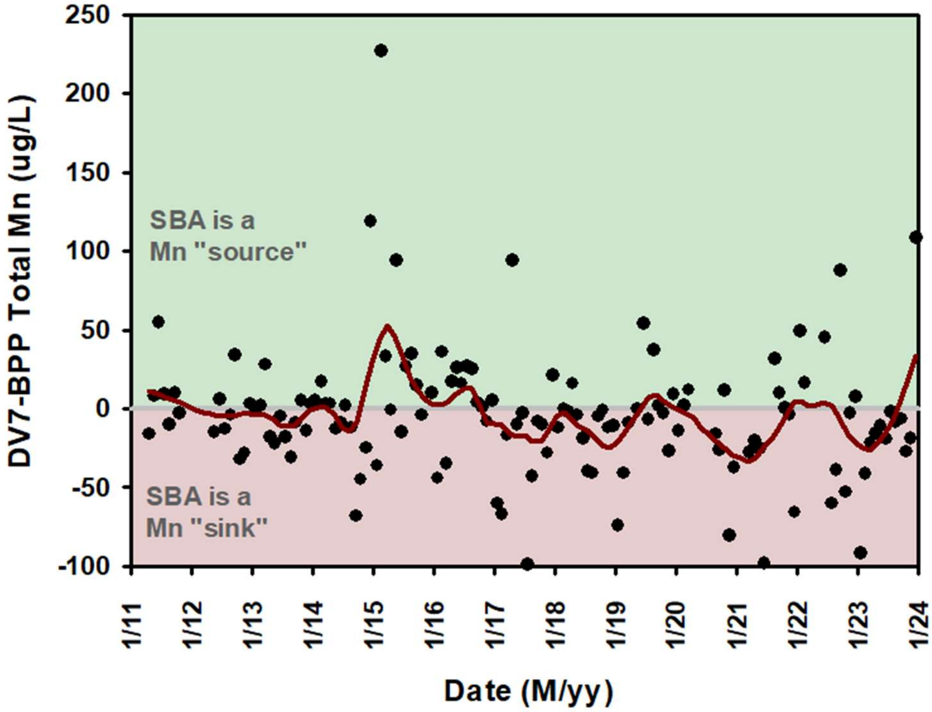

Figure 24 - Time series of the difference between paired monthly total Mn values for DV7 and BPP. Positive values (DV7>BPP) indicate that infrastructure downstream of BPP is acting as a source of Mn to DV7 while negative values indicate that this infrastructure is acting as a sink. Trend line is fitted using LOESS regression.

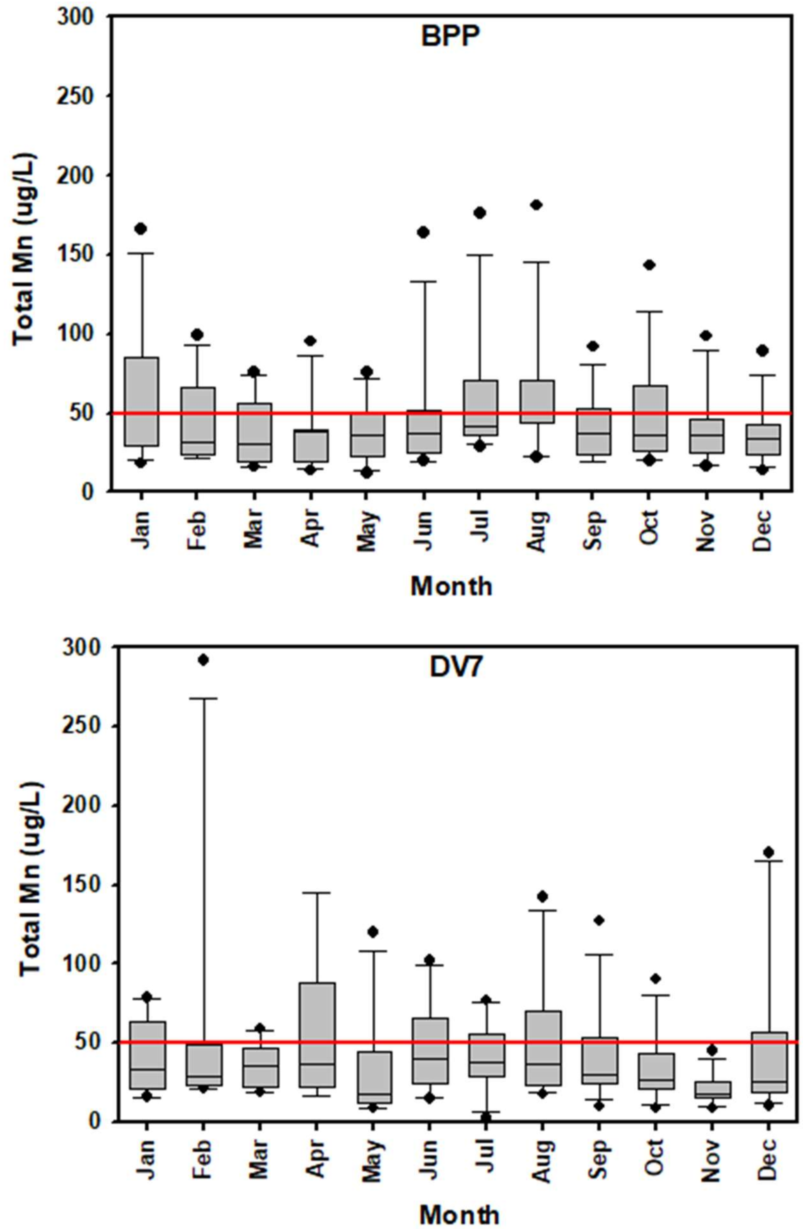

Figure 25 - Box plots of monthly total Mn data at BPP and DV7 for each calendar month. See General Methods *for explanation of box plot interpretation. Red horizontal line is the 50 ug/L total Mn secondary standard.*

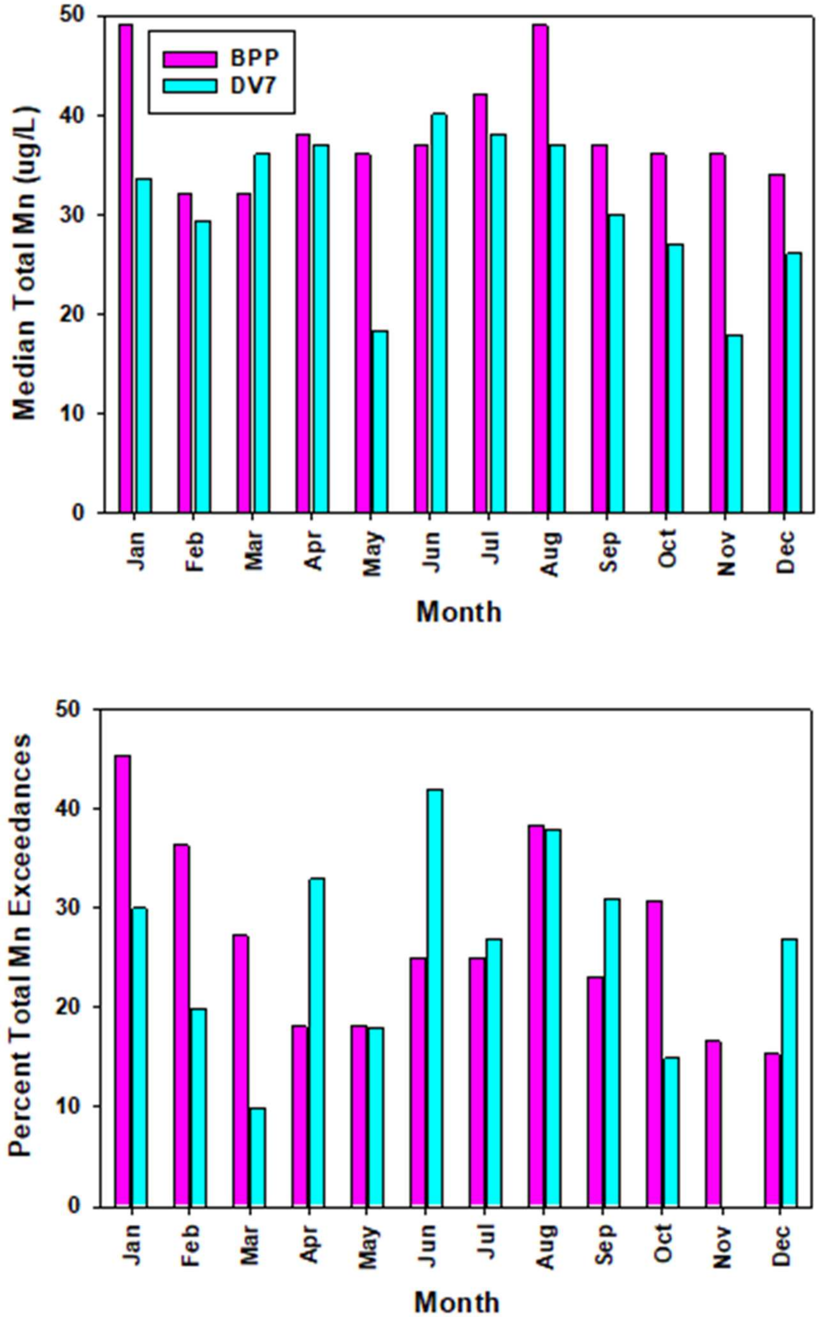

Figure 26 - Median total Mn concentrations and the percentage of years when exceedances (total Mn >50 ug/L) occurred during each calendar month at BPP and DV7.

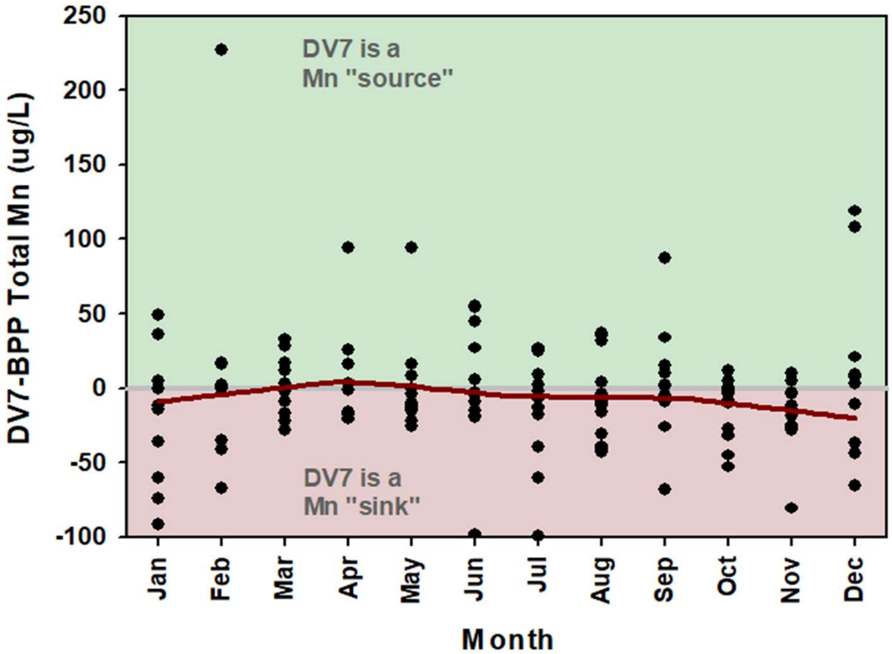

Figure 27 - Differences between paired monthly total Mn values for DV7 and BPP for each calendar month. Positive values (DV7>BPP) indicate that infrastructure downstream of BPP was acting as a source of Mn to DV7 while negative values indicate that this infrastructure was acting as a sink. Trend line is fitted using LOESS regression.

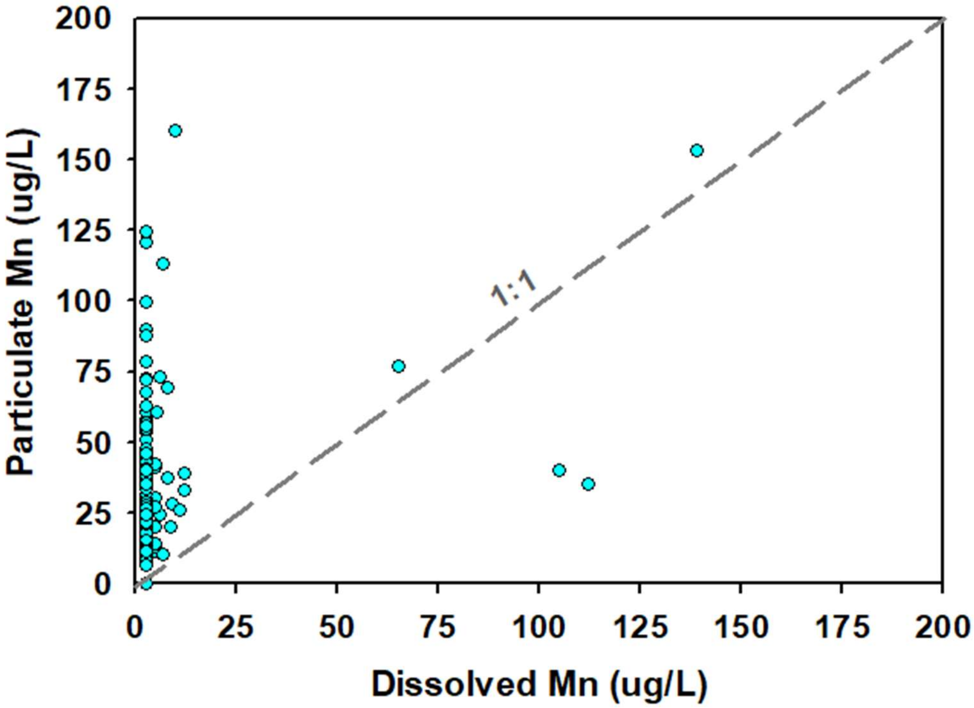

Figure 28 -Paired monthly dissolved (measured) and particulate (calculated) Mn concentrations at DV7. Dashed 1:1 line separates samples composed mostly of particulate Mn (upper left area) and those that are mostly dissolved Mn (lower right area).

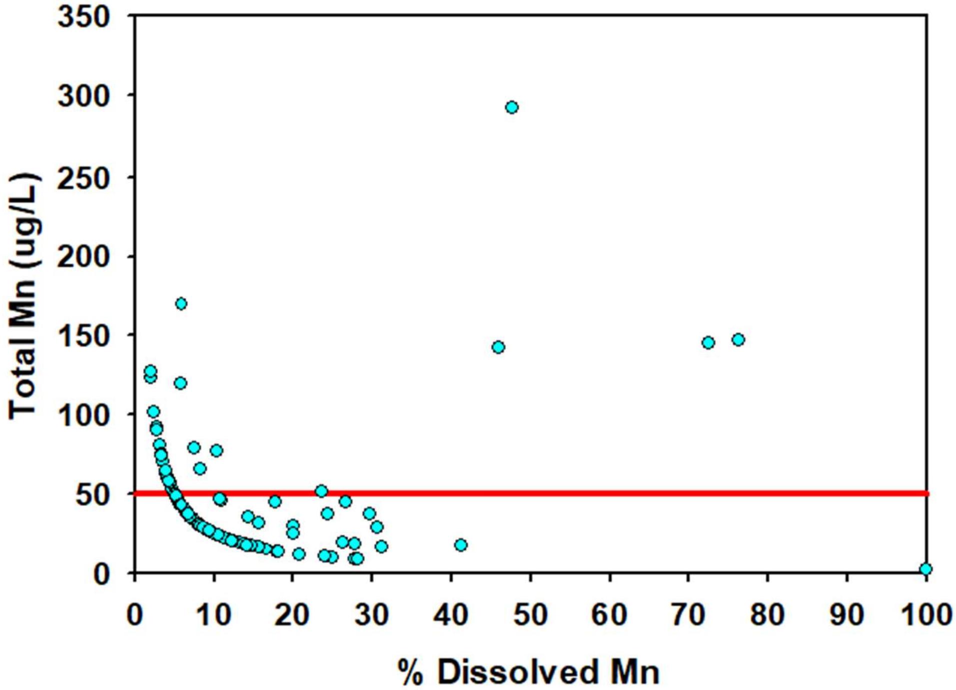

Figure 29- Percentage contribution of dissolved Mn to total Mn concentrations at DV7. Red horizontal line is the 50 ug/L total Mn secondary standard.

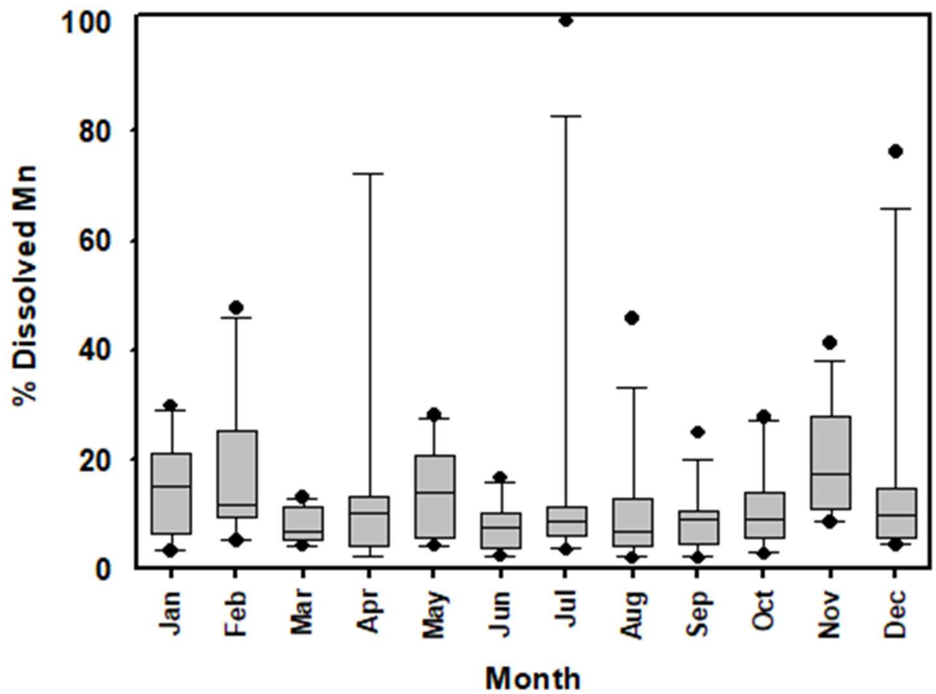

Figure 30 - Box plots of the percentage contribution of dissolved Mn to monthly total Mn concentrations at DV7 for each calendar month. See General Methods *for explanation of box plot interpretation.*

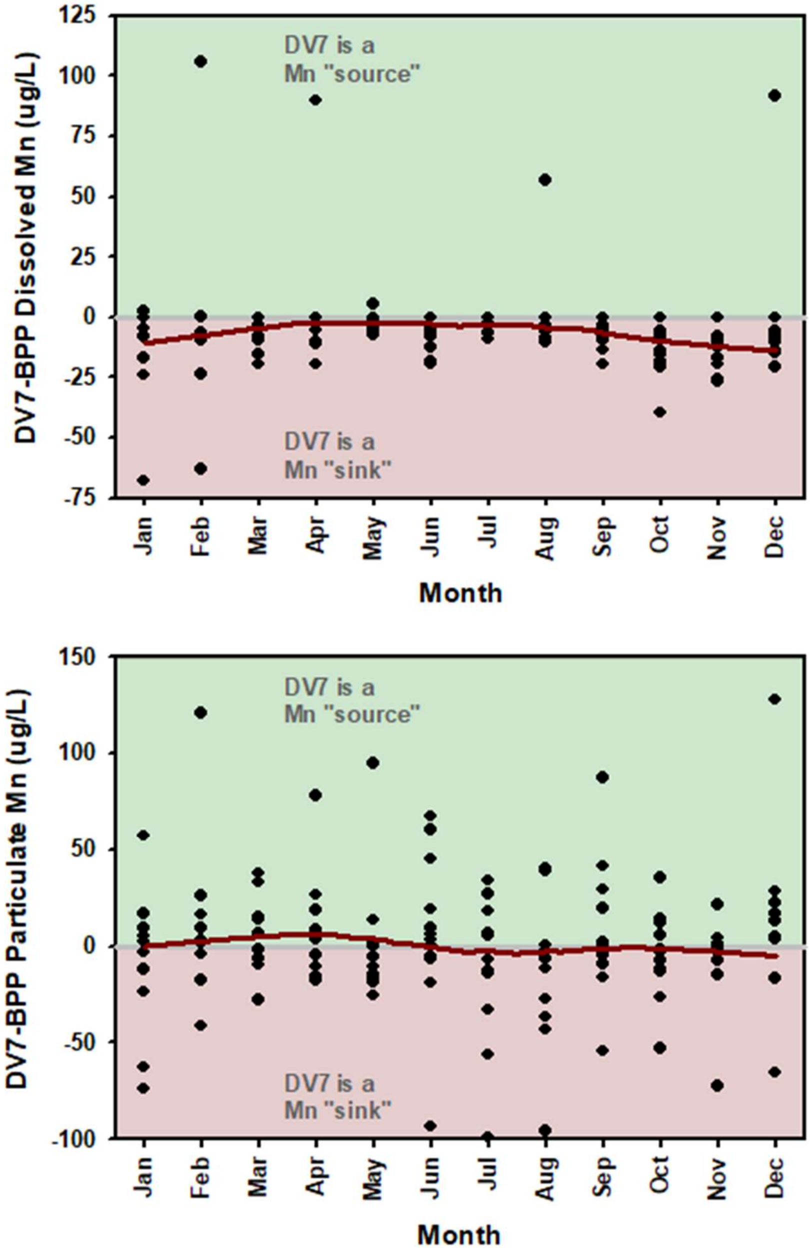

Figure 31 - Differences between paired DV7 and BPP values for dissolved (top) and particulate (bottom) Mn concentrations for each calendar month. Positive values (DV7>BPP) indicate that infrastructure downstream of BPP was acting as a source for these Mn fractions to DV7 while negative values indicate that this infrastructure was acting as a sink. Trend lines are fitted using LOESS regression.

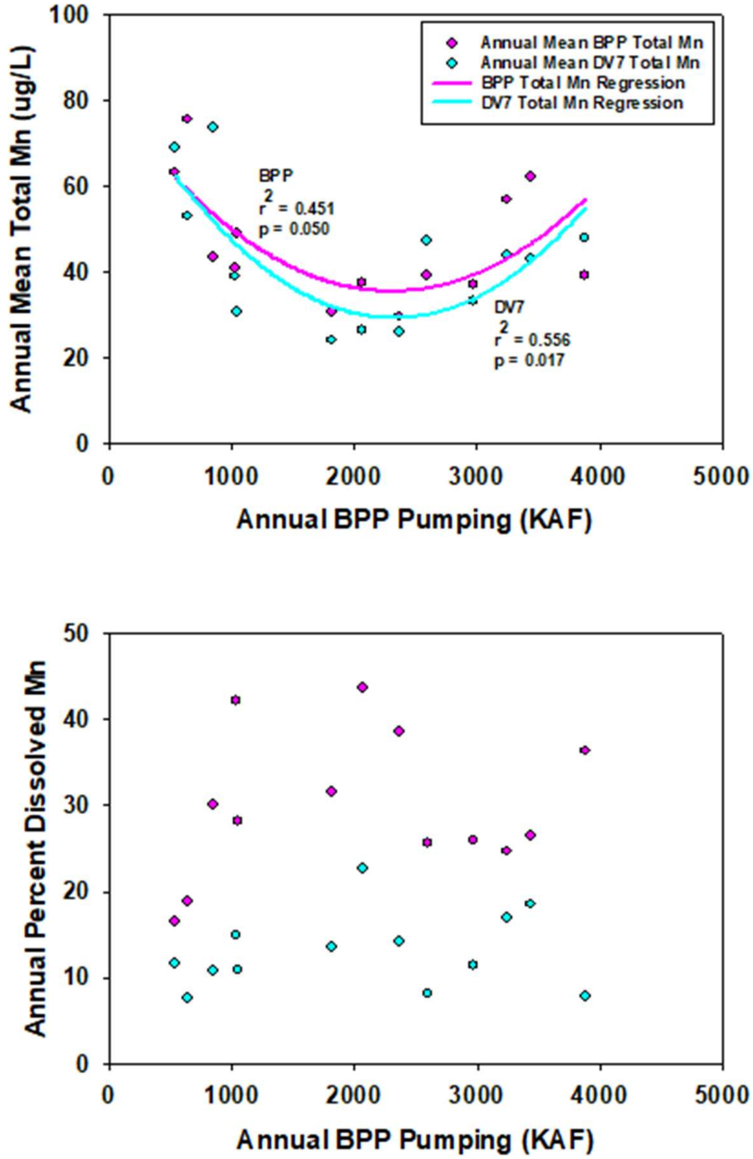

Figure 32 - Relationship between annual mean Mn concentrations and the corresponding annual pumping volume at BPP for total Mn (top) and percentage contribution of dissolved Mn (bottom) at DV7 and BPP. The best fit polynomial regression relationships are shown when significant.

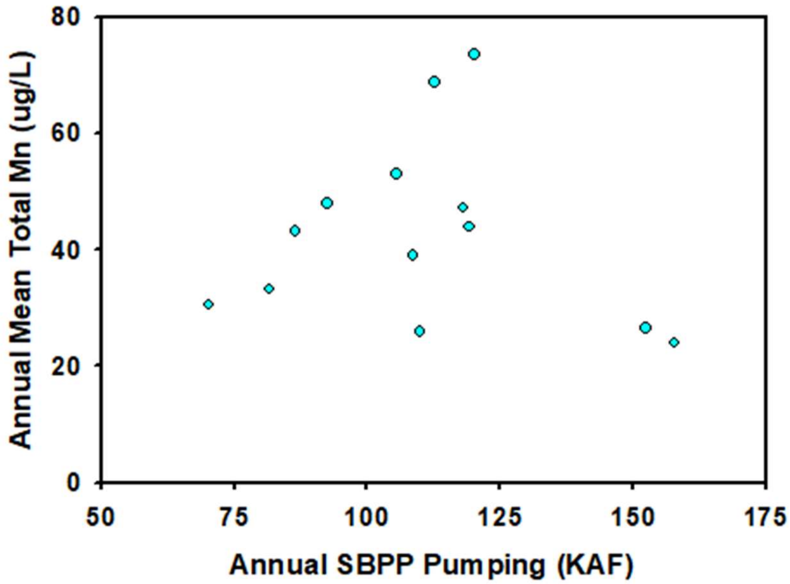

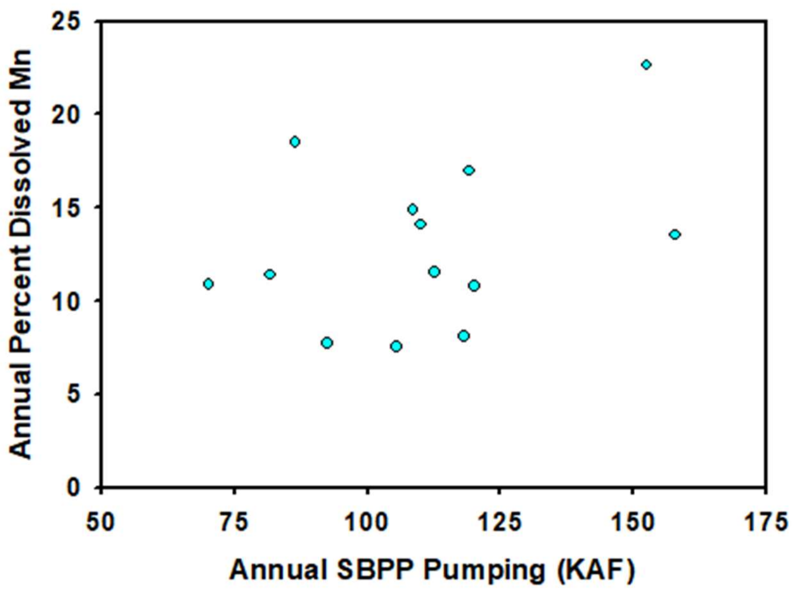

Figure 33 - Relationship between annual mean Mn concentrations and the corresponding annual pumping volume at SBPP for total Mn (top) and percentage contribution of dissolved Mn (bottom) at DV7. Polynomial regression did not detect any statistically relationship.

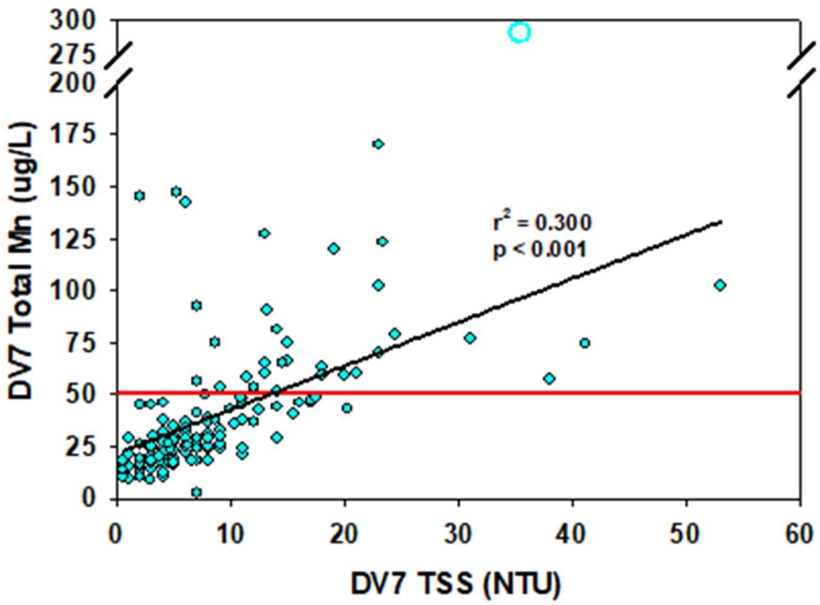

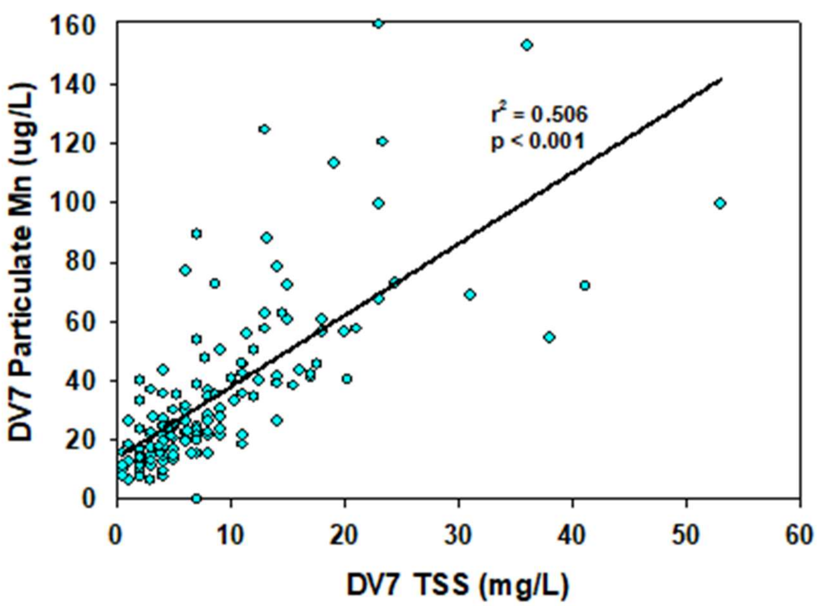

Figure 34 – Relationships between monthly total Mn (top) and particulate Mn (bottom) concentrations and total suspended solids (TSS) values at DV7. The total Mn graph includes the extreme high value (large open circle) that was not included in statistical analyses Lines show significant regression relationships. Red horizontal line is the 50 ug/L total Mn secondary standard.

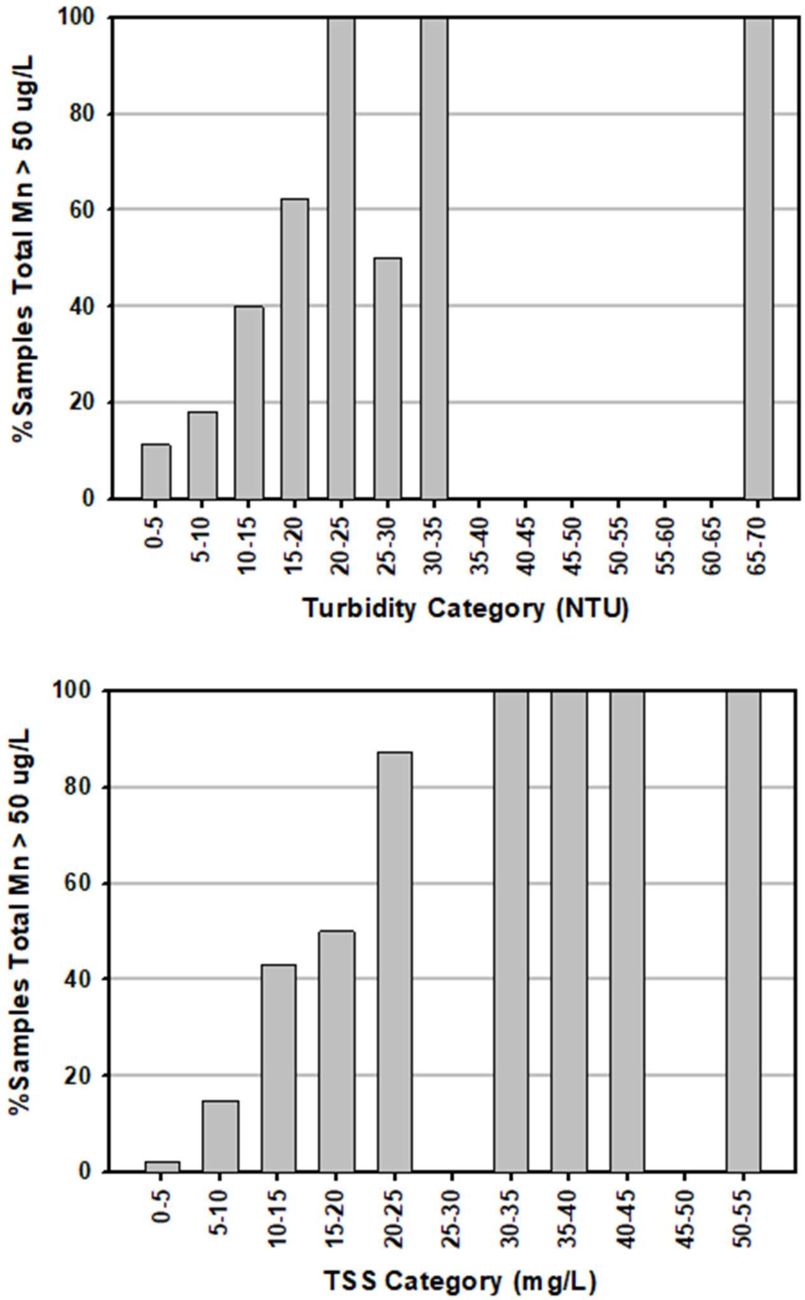

Figure 35 - Relationship between the frequency of monthly total Mn exceedances and levels of turbidity and TSS in the SBA at DV7.

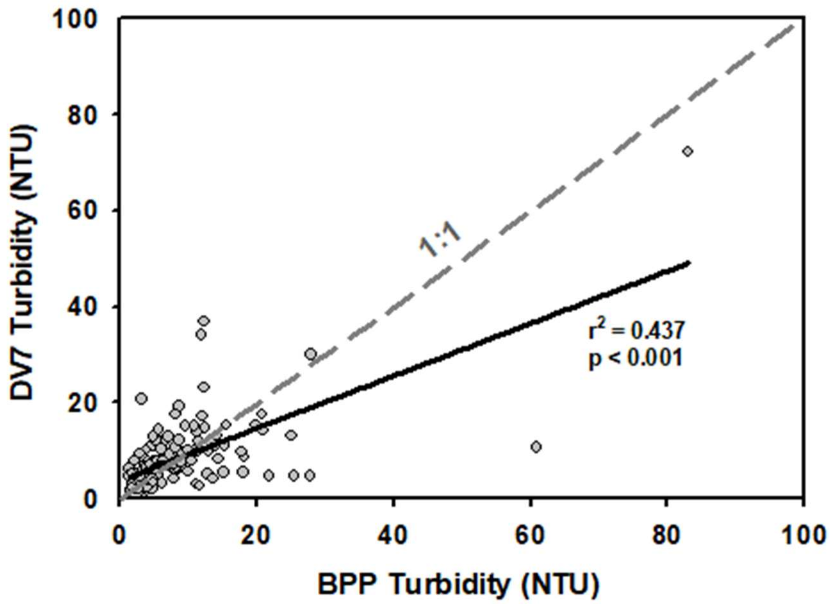

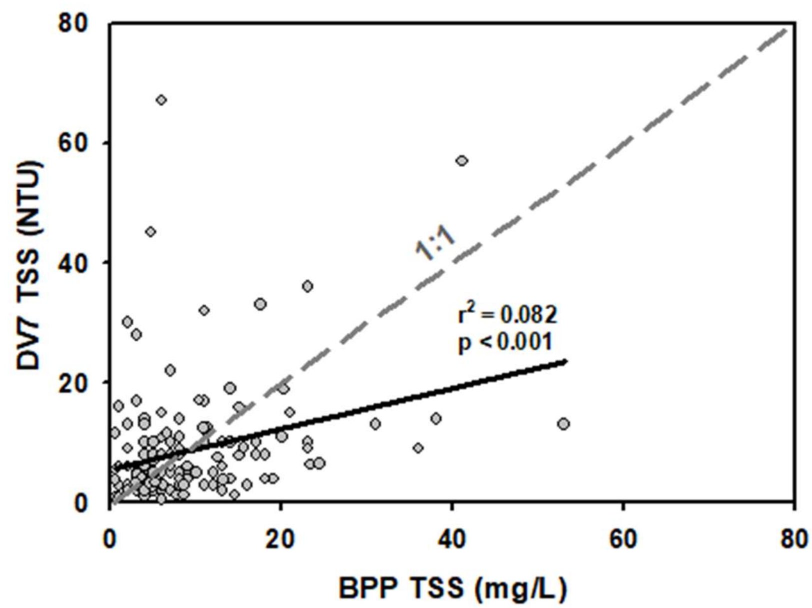

Figure 36- Relationships between monthly measures of suspended particulate matter (turbidity, TSS) at DV7 and BPP. Dashed 1:1 line separates samples where DV7 suspended matter was greater than at BPP (upper left area) and where it was lower lower (lower right area). Solid lines show significant regression relationships.

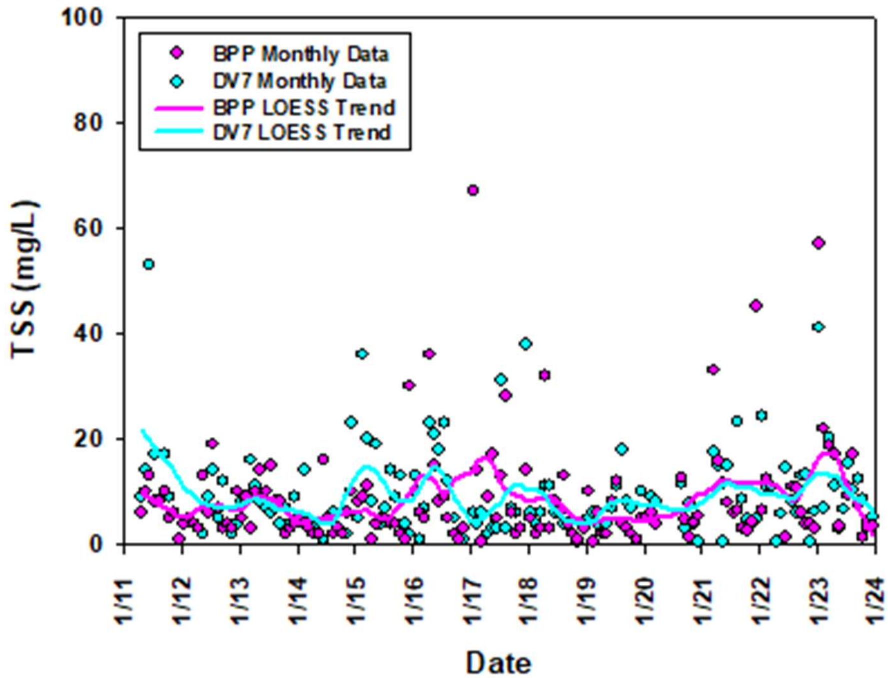

Figure 37 - Time series of monthly TSS data for BPP and DV7. Trend lines are fitted using LOESS regression.

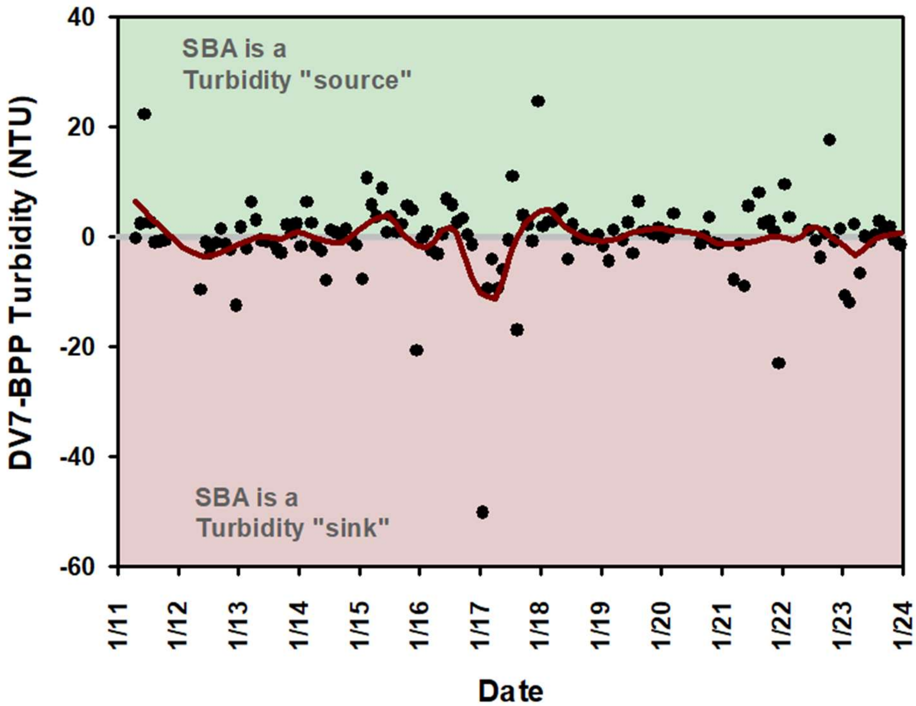

Figure 38 - Time series of the difference between paired monthly TSS values for DV7 and BPP. Positive values (DV7>BPP) indicate that infrastructure downstream of BPP is acting as a source of TSS to DV7 while negative values indicate that this infrastructure is acting as a sink. Trend line is fitted using LOESS regression.

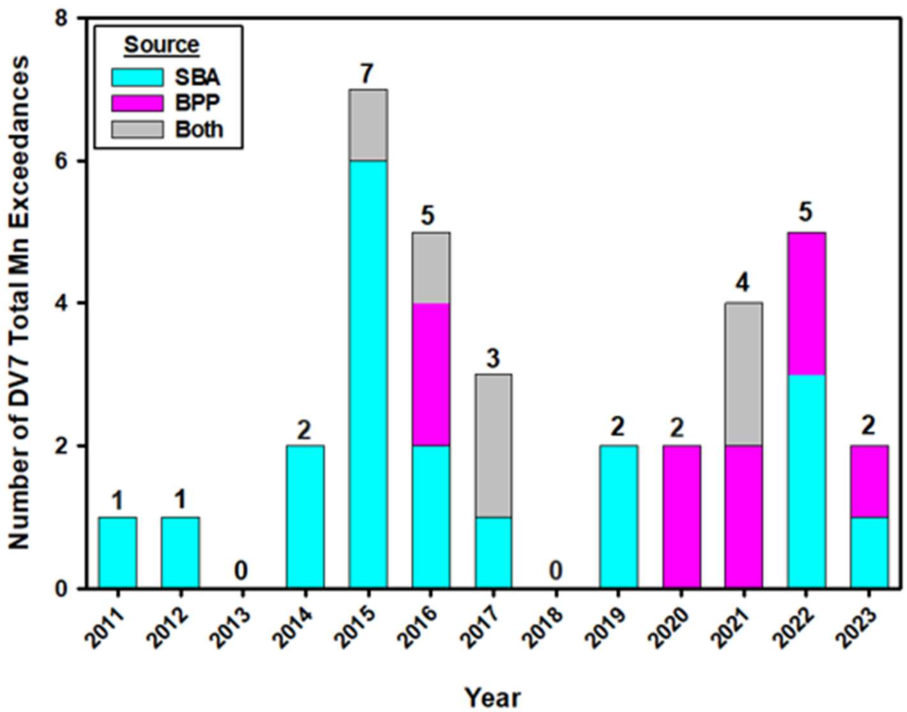

Figure 39 - Number of total Mn exceedances at DV7 for each year during the POR. The number of exceedances is shown above each bar. Using the method described in the text, each exceedance was attributed to one of three sources: 1) infrastructure downstream of BPP (SBA); 2) BPP; 3) contributions from both sources.

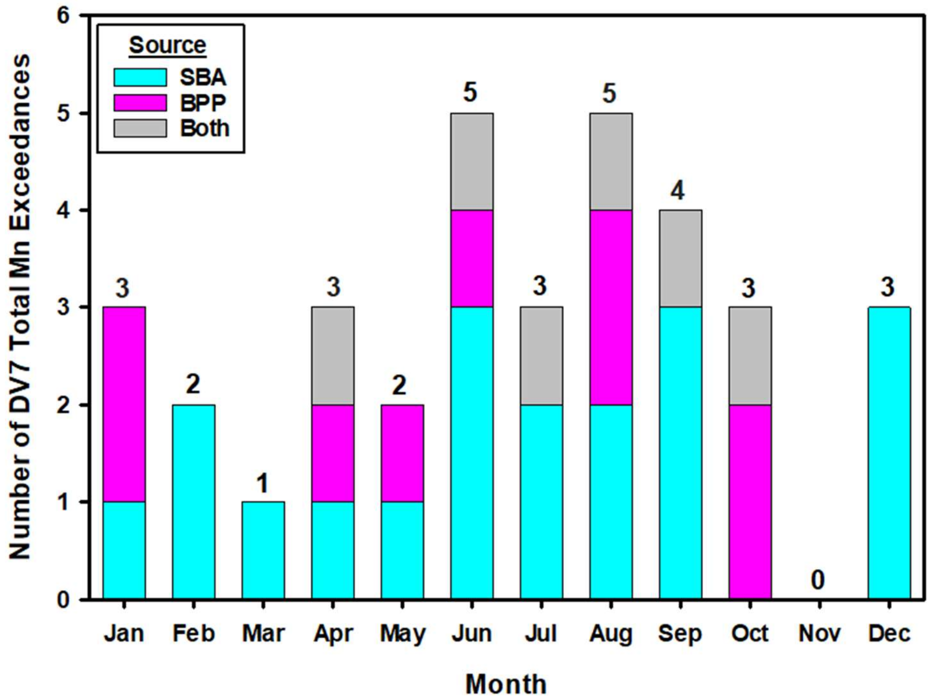

Figure 40 - Number of total Mn exceedances at DV7 for each calendar month during the POR. The number of exceedances is shown above each bar. Using the method described in the text, each exceedance was attributed to one of three sources: 1) infrastructure downstream of BPP (SBA); 2) BPP; 3) contributions from both sources.

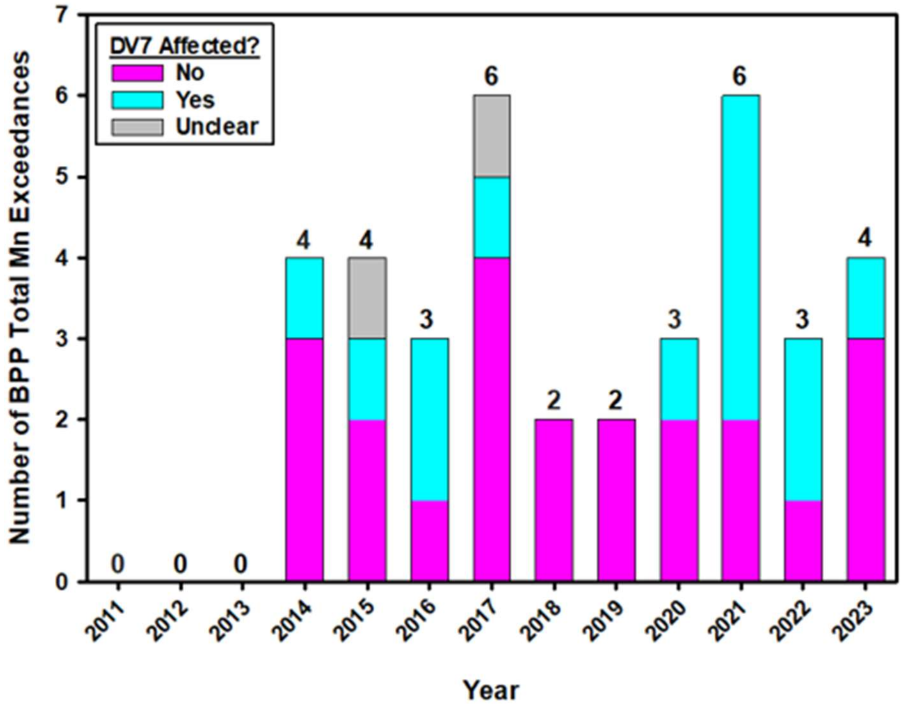

Figure 41 - Number of total Mn exceedances at BPP for each year during the POR. The number of exceedances are categorized as to whether they were associated with an exceedance at DV7 during the same sampling month.

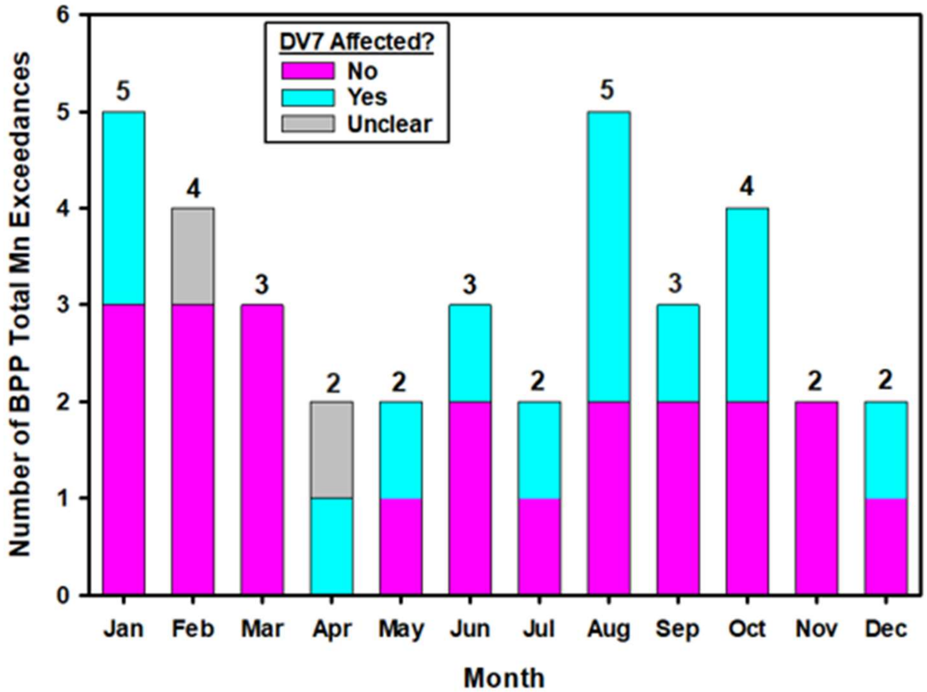

Figure 42 - Number of total Mn exceedances at BPP for each calendar month during the POR. The number of exceedances are categorized as to whether they were associated with an exceedance at DV7 during the same sampling month.

REPORT CONCLUSIONS

The goal of this analysis was to understand the sources of elevated Mn concentrations – specifically, Mn exceedances where total Mn >50 ug/L – in the section of the SWP just downstream of the Delta, including Banks Pumping Plant and the South Bay Aqueduct (Del Valle Check 7). The Delta is the external source of Mn to this part of the SWP. However, during the period 2011-2023 Mn concentrations in Delta waters entering the SWP at Clifton Court Inlet were often lower than downstream concentrations and were only a major source of SWP Mn exceedances in the wettest winters. By contrast, 79% of Banks' exceedances during that period were attributable to Mn sourced from Clifton Court Forebay and 56% of South Bay Aqueduct exceedances were attributable to Mn contributions from the SWP downstream of BPP. Therefore, Mn stored within the SWP itself appears to be the source of most Mn exceedances at Banks and in the South Bay Aqueduct.

Manganese concentration patterns identified in this analysis support the importance of Mn storage and cycling within this section of the SWP. The significant increase in total Mn concentrations at the Banks relative to Clifton Court Forebay Inlet indicates that Mn accumulation and release within the forebay has become increasingly important over time. The overall decline in Mn concentrations between Banks and Del Valle Check 7 provides evidence for Mn storage in the SWP downstream of Banks, and the finding that downstream areas are also the source of many exceedances at Del Valle Check 7 indicates that this stored Mn can be released under certain conditions. The chemical forms of Mn also change as water moves between Clifton Court Inlet and Del Valle Check 7 as most dissolved Mn is converted into particulate forms, providing further evidence of Mn reactivity in the SWP. Therefore, rather than being a passive conduit for Delta Mn, the SWP actively processes incoming Mn through biogeochemical mechanisms related to transformation, storage, and release.

Manganese is a reactive element that readily partitions among dissolved, particulate, and sediment-bound forms as environmental conditions change. As redox conditions, pH, and hydraulic conditions shift, manganese is redistributed between water, sediments, and other biogeochemical compartments. Accumulated organic and inorganic sediments within the SWP are likely a major storage compartment for Mn in forms susceptible to release under low redox (and possibly low pH) conditions. Locations such as Clifton Court, Bethany Reservoir, and check structures where sediments accumulate may, therefore, be important internal Mn sources. Aquatic vegetation is abundant at certain SWP locations such as Clifton Court and the open channel section of the South Bay Aqueduct and can also be a significant accumulator of Mn, which may be stored in plant tissue or precipitated onto leaf surfaces by Mn-oxidizing biofilms. These forms are susceptible to release upon decomposition. Plant mediated processes also may be responsible for the documented conversion of dissolved Mn to particulate forms as water flows from Banks to Del Valle Check 7, with the open-channel section of the South Bay Aqueduct being one likely location for this transformation. Other environmental compartments that have been shown to mediate Mn concentrations in engineered systems and may contribute to

Mn storage and release within the SWP include biofilms and chemical deposits attached to aqueduct and pipeline surfaces.

This analysis used monthly water-quality monitoring data over a long period of record to conclude that internal Mn sources within the SWP – rather than high Mn concentrations entering from the Delta – are the primary cause of Mn exceedances at Banks and Del Valle Check 7. However, these data alone cannot be used identify the Mn sources and operational conditions within the SWP that contribute to these exceedances. A more targeted field sampling approach is required to identify locations that are “hotspots” for Mn storage and release. For example, a 2025 study funded by the SWC analyzed sediment samples collected in Clifton Court Forebay and concluded that forebay sediments are a potentially significant source of Mn exceedances at Banks (see Appendix A for an update on this study). Likewise, sediment deposits downstream of Banks (e.g., possibly within Bethany Reservoir and the South Bay Aqueduct) may contribute to exceedances at Del Valle Check 7. Abundant aquatic vegetation in Clifton Court and the South Bay Aqueduct is another environmental compartment that can modulate Mn in downstream water based on seasonal growth habitats and vegetation management actions. Identifying the major internal sources of Mn in the SWP – their location and susceptibility to release under different environmental conditions – would help to identify the causes of Mn exceedances documented in this report and allow for the development of operational and other management strategies for mitigating Mn problems.

LITERATURE CITED

Brandhuber, P. 2013. Legacy of Manganese Accumulation in Water Systems. Literature Review. Water Research Foundation Report. 43 p.

MacWilliams, M.L., and E.S. Gross. 2013. Hydrodynamic Simulation of Circulation and Residence Time in Clifton Court Forebay. San Francisco Estuary and Watershed Science 11(2):1-30.

Shrestha, B.P., and S. Adil. 2019. Clifton Court Forebay In-Depth Dredging Analysis. California Department of Water Resources Bay Delta Office. 318 p.

APPENDIX A: CLIFTON COURT FOREBAY SEDIMENT STUDY: PRELIMINARY FINDINGS

Author: Paul McCormick (external collaborators: Marc Beutel, UC-Merced, and Patrick Inglett, University of Florida)

Date: January 2026

Clifton Court Forebay (CCF) sediments are a likely source of nutrients and manganese (Mn) that affect downstream utilities. Sediment releases of these constituents are likely affected by sediment oxygen levels, which are determined by the relative rates of oxygen diffusion (supply) and microbial activity (demand). Forebay sediments were sampled in April 2025 to quantify nutrient and Mn concentrations and the potential for their release to the water supply when oxygen is present (oxic) and absent (anoxic). A laboratory experiment was also conducted to quantify these releases under different oxygen conditions. The following preliminary findings relate to conditions at the time of sampling and do not account for seasonal and hydrologic variability that likely affect sediment conditions.

Forebay sediments were fairly dense, which may limit oxygen supply, but also had a fairly low organic matter content, which may limit microbial oxygen demand. Oxygen levels in the sediments were not measured, but the mottled coloration of some sediments indicated at least the periodic occurrence of anoxia. Turbulent (high flow and wave action) locations on the SE and E side of the forebay had denser sediments with less organic matter compared to locations on the W and N sides. These differences may affect nutrient and Mn storage and release patterns within CCF.

Sediment nutrient characteristics (e.g., total C:N:P ratios skewed towards surplus P availability, low microbial biomass C and N) suggest (but do not *prove*) that microbial activity was limited by C and/or N availability rather than by P at the time of sampling. This is consistent with the fact that C and N availability is closely tied to sediment organic matter content, which is fairly low in CCF, while P availability is also influenced by inorganic forms such as metal-bound P. Two major nutrient gradients were identified in the forebay: 1) an organic CNP gradient aligned with the "turbulence" gradient described above; 2) an inorganic P gradient associated with sediment Mn concentrations. While organic-bound nutrients can be released under both oxic and anoxic conditions, metal-bound inorganic P is stored under oxic conditions and released under anoxic conditions.

Sediment Mn concentrations were fairly high, and about 85% of sediment Mn was potentially available for release as dissolved Mn, mostly under anoxic conditions. A strong correlation between sediment metal-bound P and Mn indicates that Mn-bound P is an important store of sediment P that is dissolved during anoxia, releasing both elements simultaneously. Sediment resuspension due to turbulence – apparently common in CCF – could be another important source of dissolved and particulate Mn that is independent of oxygen influences and was not measured during this sampling event.

The laboratory experiment measured the release of dissolved P (phosphate), N (ammonia), and Mn (Mn^{2+}) from sediments at 4 sites when incubated under oxic, hypoxic (low oxygen), and anoxic conditions. Releases of all three constituents were moderate when compared to data from a range of other CA reservoirs. Phosphate was released under all oxygen conditions with the highest releases during the anoxic phase. Ammonia releases were limited to the hypoxic and anoxic phases, again with highest releases during anoxia. Manganese releases were limited to the anoxic phase. These results are consistent with sediment release patterns in other reservoirs showing that periods of sediment anoxia increase nutrient and Mn concentrations in the overlying water. The release of phosphate from the sediment even under oxic conditions also supports other indications of surplus P (described above).

These preliminary findings confirm that CCF sediments are both a store and a source of nutrients and Mn within the SWP. Sediment characteristics reflect that this shallow forebay experiences frequent turbulent conditions that limit deposition of lighter organic matter in favor of heavier inorganic material. This condition may constrain organic nutrient sources while allowing for accumulation of P and Mn in inorganic complexes that are susceptible to release under anoxic conditions. Despite frequent turbulence aerating the overlying water column, the high sediment density and coloration patterns indicate that sediments can become anoxic at times, and the experimental evidence presented here shows that sediment anoxia results in releases of dissolved P, N, and Mn. Resuspension of unconsolidated sediments caused by flow and wave action may be another pathway for release of these constituents (in both dissolved and particulate forms) unrelated to sediment oxygen.

A final report is in progress and will include:

1) Additional and more detailed (statistical and graphical) results;
2) Estimates of how measured releases translate into concentrations at Banks Pumping Plant;
3) Comparisons with other CA reservoirs that experience similar nutrient and Mn water-quality issues;
4) Data gaps and additional measurements that could resolve them (e.g., significance of sediment resuspension as a release pathway, importance of seasonal organic matter inputs (submerged vegetation and cyanobacteria growth in CCF) on storage and release).